Oncology and Translational Medicine

Volume 6 • Number 3 • June 2020

Oncology and Translational Medicine Volume 6 • Number 3 • June 2020 pp 93-133

邮发代号：38-121
ISSN 2095-9621

GENERAL INFORMATION
≫otm.tjh.com.cn

ISSN 2095-9621
CN 42-1865/R

Oncology and Translational Medicine

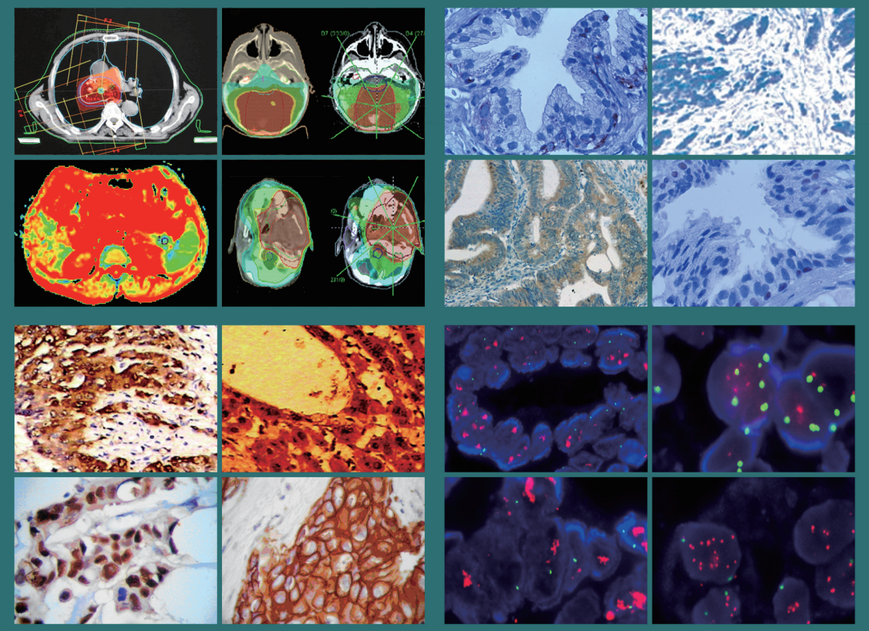

Volume 6
Number 3
June 2020

Oncology and Translational Medicine

Oncology and Translational Medicine
June 2020 Volume 6 Number 3

Contents

Oncology and Translational Medicine

Aims & Scope

Oncology and Translational Medicine is an international professional academic periodical. The Journal is designed to report progress in research and the latest findings in domestic and international oncology and translational medicine, to facilitate international academic exchanges, and to promote research in oncology and translational medicine as well as levels of service in clinical practice. The entire journal is published in English for a domestic and international readership.

Copyright

Supervised by

Ministry of Education of the People's Republic of China.

Administered by

Tongji Medical College, Huazhong University of Science and Technology.

Submission information

Manuscripts should be submitted to:
http://otm.tjh.com.cn
dmedizin@sina.com

Subscription information

ISSN edition: 2095-9621
CN: 42-1865/R

■ Subscription rates
Subscription may begin at any time. Remittances made by check, draft or express money order should be made payable to this journal. The price for 2020 is as follows: US $ 30 per issue; RMB ￥28.00 per issue.

Database

Oncology and Translational Medicine is abstracted and indexed in EMBASE, Index Copernicus, Chinese Science and Technology Paper Citation Database (CSTPCD), Chinese Core Journals Database, Chinese Journal Full-text Database (CJFD), Wanfang Data; Weipu Data; Chinese Academic Journal Comprehensive Evaluation Database.

Business correspondence

All matters relating to orders, subscriptions, back issues, offprints, advertisement booking and general enquiries should be addressed to the editorial office.

Mailing address
Editorial office of
Oncology and Translational Medicine
Tongji Hospital
Tongji Medical College
Huazhong University of Science and Technology
Jie Fang Da Dao 1095
430030 Wuhan, China
Tel.: +86-27-69378388
Email: dmedizin@sina.com

Printer
Changjiang Spatial Information Technology Engineering Co., Ltd. (Wuhan) Hangce Information Cartorgraphy Printing Filial, Wuhan, China
Printed in People's Republic of China

Managing director

Jun Xia

Executive editors

Oncology and Translational Medicine
DOI 10.1007/s10330-020-0404-4

June 2020, Vol. 6, No. 3, P93–P97

ORIGINAL ARTICLE

Application of biological optimization of hypofractionated radiotherapy post conservative surgery for breast cancer*

Ying Shao [1, 2], Yadi Wang [1], Fuli Zhang [1] (✉), Shi Wang [3]

[1] Department of Radiotherapy, The Seventh Medical Center, PLA General Hospital, Beijing 100700, China
[2] Department of Radiotherapy, Beijing Tsinghua Changgung Hospital affiliated to Tsinghua University, Beijing 102218, China
[3] Department of Engineering Physics, Tsinghua University, Beijing 100084, China

Abstract

Objective The aim of the study was to discuss the application of biological optimization and its difference from physical optimization in hypofractionated radiotherapy for breast cancer after conservative surgery.
Methods This retrospective study enrolled 15 randomly chosen patients with left-sided breast cancer who received radiotherapy. The volumetric arc therapy (VMAT) technique was used to redesign treatment plans with physical functions (PF) group, biological-physical functions combined (BF + PF and PF + BF) groups, and biological functions (BF) group. The dosimetric differences based on the above four optimization methods were assessed by calculating and analyzing the corresponding dose-volume parameters.
Results The target parameters of the four groups differed significantly ($P < 0.05$) except for the conformity index (CI). The tumor control probability (TCP) values in the BF and BF + PF groups were higher than those in the PF and PF + BF groups. Moreover, the dose-volume parameters of the ipsilateral lung in the BF group were less than those of three other groups, while the monitor unit (MU) in the BF group was approximately 16% lower than those of the PF and PF + BF groups.
Conclusion Biological functions were useful to increase the equivalent uniform dose (EUD) and TCP values of the target, decrease the dose-volume parameters of the organs-at-risk (OARs), and improve treatment efficiency.

Received: 26 January 2020
Revised: 24 February 2020
Accepted: 6 March 2020

Key words: equivalent uniform dose (EUD); breast cancer; hypofractionated radiotherapy; dosimetry

In routine radiotherapy work, medical physicists achieve accurate dose calculations utilizing various treatment planning systems (TPS), which provide different types of optimization functions and algorithms to meet clinical dosimetry requirements. The physical function based on dose-volume parameters is simple and straightforward to use for the optimization of intensity-modulated radiotherapy (IMRT); however, its main disadvantage is that it does not reflect nonlinear responses of tumors and normal tissues to irradiation. By only utilizing a physical function to a certain point on the dose curve [1], the overall dose distribution of the target or organs-at-risk (OARs) cannot be adjusted; thus, it has certain limitations in constraining the overall dose to the tissue. The biological function based on the equivalent uniform dose (EUD) includes biological parameters reflecting the interaction between radiation and tissue, which can offset the limitations of the sole physical function optimization. Research and reports on breast cancer hypofractionation radiotherapy have confirmed that this treatment mode can achieve an equivalent effect to that for conventional fractionation, reducing the total cost to patients [2–6]. The present study evaluated the effects of different biological parameters on target EUD and tumor control probability (TCP) by comparing treatment plan optimization results based on physical functions (PF group), the combination of physical and biological functions (BF + PF and PF + BF groups), and

✉ Correspondence to: Fuli Zhang. Email: radiozfli@163.com
* Supported by a grant from the Beijing Municipal Science and Technology Commission (No. Z181100001718011).

biological functions (BF group), providing a dosimetric reference for clinical application.

Materials and methods

Patient data

Computed tomography (CT) scans from 15 patients with left-sided breast cancer (T1N0 carcinoma) treated at our hospital (The Seventh Medical Center, PLA General Hospital, Beijing, China) between July 2007 and January 2016 were analyzed. The median patient age was 55 (range: 33–63) years. The patients were placed in the supine position on a breast board (Med Tec, Orange City, IA) with both arms raised above their head and sternum parallel to the couch. Lead wires were placed to locate the breast, scar, and skin marks on the CT images. The patients were scanned from the level of the larynx to the level of the upper abdomen, including the left and right lungs, with 5-mm slice thickness and slice separations.

Target volumes

The delineation of target and critical structures for all patients was done by a single radiation oncologist with extensive experience in breast cancer treatment. The clinical target volumes (CTVs) included the breast defined as the glandular tissue apparent on CT scan, while the planning target volumes (PTVs) included the breast parenchyma with a 3-mm rim of the skin removed. Retraction of the breast contour 3-mm from the skin surface was used to account for dose build-up during dose calculation.

OARs

The OARs included the left and right lungs, the heart, and the contralateral breast. The esophagus, thyroid, and humeral head, though not mentioned in the following dose distribution analysis in this work, were also delineated.

Methods

The EUD is a concept of biological dose related to the biological characteristics of tissues proposed by Niemierko *et al* [7–8]. The EUD combines the physical dose with the TCP and normal tissue complication probability (NTCP) [8]. The most common formula is as follows:

$$EUD = \left(\frac{1}{N}\sum_{i=1} D_i^{a}\right)^{\frac{1}{a}} \quad (1)$$

where N is the number of voxels in the region of interest (ROI), D_i is the dose of the ith voxel in the ROI, and a is a biological parameter describing the dose-volume effect of the tumor or normal tissue. For tumors, a is usually a negative value with a larger absolute value; for serial OARs, a is usually a positive value with a larger absolute value; for parallel OARs, a is usually a positive value with a smaller absolute value [9–10]. In this study, to clearly show the relationship between the a value and the dose responses of the targets and normal lung tissues, the a value of the targets ranged from –100 to –10 with intervals of 10; for normal lung tissues, the a value ranged from 0.1 to 1.0 with intervals of 0.1 [11].

The TCP model is a logical model proposed by Bentzen *et al* [12], as follows:

$$TCP = \frac{1}{1+\left(\frac{TCD_{50}}{EUD}\right)^{4\gamma_{50}}} \quad (2)$$

where TCD_{50} is the dose required when the tumor control rate reaches 50% and γ_{50} is the slope of the tumor tissue dose-response curve. TCD_{50} and γ_{50} are both obtained from large quantities of clinical data.

The NTCP model is based on the assumption that there is no volume effect between voxels of normal tissues [10] and has a formula similar to that for TCP:

$$NTCP = \frac{1}{1+\left(\frac{TD_{50}}{EUD}\right)^{4\gamma_{50}}} \quad (3)$$

where TD_{50} is the dose required when the NTCP reaches 50% and γ_{50} is the slope of the dose-response curve of normal tissue and can be taken as $\frac{1}{m\sqrt{2\pi}}$, where m is a parameter related to the slope of the dose-response curve obtained from clinical data [12].

Designing treatment plans

CT images of 15 patients with left breast cancer receiving radiation therapy were chosen and volumetric arc modulation (VMAT) plans were redesigned on a Monaco 5.11 TPS (ElektaAB, Stockholm, Sweden). For each case, four plans were redesigned. First, both the target and the OARs were constrained by physical functions (PF group); second, the target was constrained by physical functions while the OARs were constrained by biological functions (PF + BF group); third, the target was constrained by biological functions while the OARs were constrained by physical functions (BF + PF group); fourth, both the target and OARs were constrained by biological functions (BF group). The prescription was set to 42.9 Gy/13 f [13], with at least 95% of the target volume surrounded by the prescribed dose. Two partial arcs of 200° were used with a starting angle of 150° an interval angle of 20° and a calculation uncertainty of 1%. When the four groups of plans were optimized, the same constraint parameters were selected.

Calculations and statistical analysis

Based on the dose-volume histogram (DVH) data derived from the treatment plan, MATLAB (version

2015a, MathWorks, US) was used to calculate: (1) the EUD and TCP values of the targets for each group for *a* values from –100 to –10 at intervals of 10; (2) the NTCP values of normal lung tissues for *a* values from 0.1 to 1.0 at intervals of 0.1. In addition, the homogeneity index (HI) and the conformity index (CI) of the target were also calculated and compared.

The calculation formula for HI was:

$$HI = \frac{D_{2\%} - D_{98\%}}{D_{50\%}} \times 100\% \quad (4)$$

in which $D_{2\%}$ approximately represents the maximum dose in the target, $D_{98\%}$ represents the minimum dose in the target, and $D_{50\%}$ is the median dose of the target.

The calculation formula for CI was:

$$CI = \frac{V_{T,Pi}}{V_T} \times \frac{V_{T,Pi}}{V_{Pi}} \quad (5)$$

where $V_{T,Pi}$ represents the target volume surrounded by the prescription dose, V_T represents the target volume, and V_{Pi} represents the total volume surrounded by the prescription dose [14].

One-way analysis of variance (ANOVA) was performed using IBM SPSS Statistics for Windows version 20.0 to analyze differences among groups; least significant difference (LSD) tests were used to analyze the differences between any two groups. Differences were considered statistically significant for $P < 0.05$.

Results

Target

The target indices are listed in Table 1. Except for CI, the differences among HI, MU, and beam-on time were statistically significant ($P < 0.05$). In addition, further LSD tests showed that the HIs of the target in the BF and the BF + PF groups were slightly worse than those in the other two groups (both $P < 0.05$); while the MU was significantly reduced, that in the BF group was reduced by about 16% compared to those in the PF and PF + BF groups (both $P < 0.05$). Therefore, the two groups of plans using biological functions had higher delivery efficiency.

Table 2 lists the EUD values of the targets of the four groups with the value of *a* ranging from –100 to –10. Only when *a* was set to –10 were significant differences observed among the four groups ($P < 0.05$). Further LSD tests showed that the EUD of the BF group was slightly higher than those of PF and PF + BF groups (both $P < 0.05$).

We also calculated and analyzed the target TCP of the four groups. Fig. 1 shows the relationship between the value of *a* and the target TCP.

OARs

Fig. 2 shows the transverse isodose distributions of the four planning groups in a single patient. The dose gradient of the BF group was larger than those of other three groups; the dose line is more compact and the ipsilateral lung received a smaller dose.

Fig. 3 shows a DVH diagram of the four groups of plans for a single patient. The DVH curve of the PTV in the BF group was significantly shifted to the right, while

Table 1 Indices of the target for the four groups of plans ($\bar{\chi} \pm s$)

Index	PF group	PF + BF group	BF group	BF + PF group	*P* value	*F* value
HI	0.097 ± 0.010	0.095 ± 0.009	0.113 ± 0.013	0.111 ± 0.009	0.000	11.610
CI	0.829 ± 0.031	0.828 ± 0.025	0.852 ± 0.028	0.843 ± 0.025	0.061	2.603
MU	1209.63 ± 111.77	1200.39 ± 166.03	1006.75 ± 57.22	1069.84 ± 105.54	0.000	10.952
BeamOn (min)	3.37 ± 0.37	3.37 ± 0.35	2.96 ± 0.32	3.09 ± 0.30	0.002	5.769

Table 2 EUD of the target ($\bar{\chi} \pm s$)

a value	PF group (Gy)	PF + BF group (Gy)	BF group (Gy)	BF + PF group (Gy)	*P* value	*F* value
–100	45.48 ± 6.76	45.33 ± 6.41	45.79 ± 7.20	45.28 ± 6.99	0.997	17.299
–90	45.95 ± 6.73	45.80 ± 6.37	46.27 ± 7.18	45.77 ± 6.98	0.997	0.405
–80	46.54 ± 6.69	46.37 ± 6.31	46.86 ± 7.16	46.36 ± 6.96	0.997	0.097
–70	47.27 ± 6.63	47.09 ± 6.21	47.60 ± 7.12	47.11 ± 6.92	0.997	0.041
–60	48.18 ± 6.51	48.02 ± 6.07	48.56 ± 7.06	48.09 ± 6.85	0.996	0.026
–50	49.30 ± 6.28	49.19 ± 5.82	49.80 ± 6.93	49.38 ± 6.72	0.994	0.020
–40	50.61 ± 5.84	50.62 ± 5.38	51.26 ± 6.57	51.02 ± 6.45	0.989	0.018
–30	51.97 ± 5.01	52.06 ± 4.57	52.76 ± 5.71	52.70 ± 5.70	0.961	0.017
–20	53.21 ± 3.43	53.27 ± 2.99	54.35 ± 3.95	54.19 ± 4.08	0.750	0.017
–10	54.31 ± 0.62	54.26 ± 0.54	55.72 ± 0.82	55.50 ± 0.85	0.000	0.017

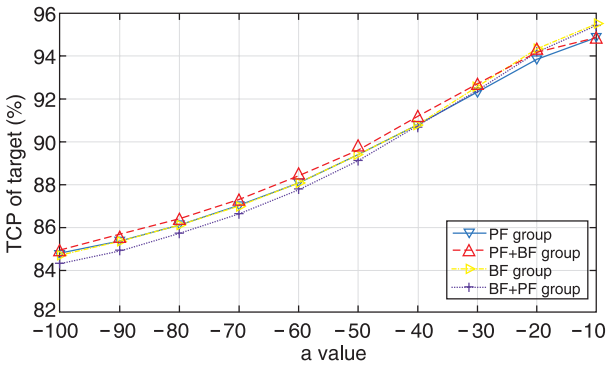

Fig. 1 Relationship between TCP and *a* value of the target

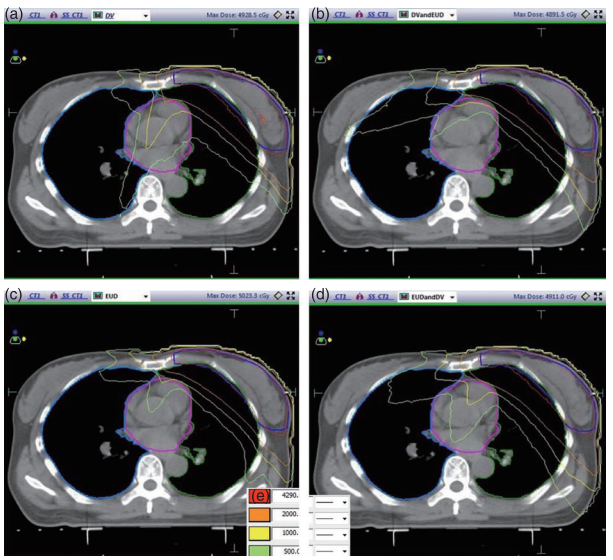

Fig. 2 Transverse isodose distributions of the four groups of plans in a single patient. (a–d) Dose distributions in the PF, PF + BF, BF and BF + PF groups, respectively; (e) Color sketch of the isodose line

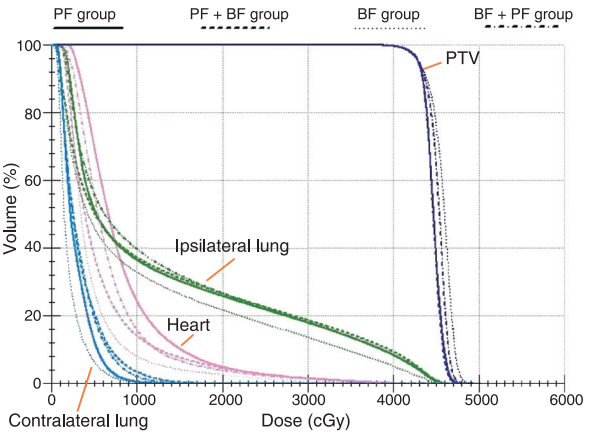

Fig. 3 DVH of the four groups for a specific patient

the DVH curves of the bilateral lung and heart were significantly shifted to the left.

Table 3 shows the dose-volume parameters of the lung and heart obtained using the four optimization methods. The irradiated dose of the ipsilateral lung and heart in the EUD group is lower than those of the other three groups. Significant differences in the ipsilateral lung V_5, V_{10}, and V_{30}; D_{mean}; and heart V_{20} were observed among the four groups ($P < 0.05$). LSD tests demonstrated a lower ipsilateral lung V_5 in the BF group compared to those in the other three groups ($P < 0.05$ for all). The ipsilateral lung V_{10} and D_{mean} in the BF group were lower than those of the PF and PF + BF groups (all $P < 0.05$). The ipsilateral lung V_{20} and V_{30} in the BF group were lower than those of the PF + BF group (all $P < 0.05$). The heart V_{20} in the BF group was lower than those of the PF and PF + BF groups (all $P < 0.05$).

Table 3 Dose-volume parameters of the organs-at-risk ($\bar{\chi} \pm s$)

Parameter	PF group	PF + BF group	BF group	BF + PF group	*P* value	*F* value
Ipsilateral lung V_5 (%)	68.19 ± 12.43	60.28 ± 6.51	52.67 ± 7.36	63.41 ± 12.15	0.001	6.387
Ipsilateral lung V_{10} (%)	39.46 ± 5.64	39.69 ± 3.95	35.19 ± 4.65	37.83 ± 4.69	0.046	2.844
Ipsilateral lung V_{20} (%)	26.21 ± 4.15	27.40 ± 3.67	24.11 ± 3.72	24.72 ± 4.32	0.111	2.096
Ipsilateral lung V_{30} (%)	19.13 ± 3.52	20.61 ± 3.16	17.21 ± 2.96	17.57 ± 3.79	0.030	3.217
Ipsilateral lung D_{mean} (Gy)	12.06 ± 1.54	12.17 ± 1.36	10.62 ± 1.40	11.34 ± 1.70	0.023	3.427
Contralateral lung V_5 (%)	24.98 ± 12.03	25.10 ± 11.52	24.21 ± 12.15	24.96 ± 9.08	0.996	0.020
Contralateral lung V_{10} (%)	5.37 ± 4.44	5.25 ± 4.26	5.15 ± 4.72	6.26 ± 4.44	0.898	0.197
Contralateral lung D_{mean} (Gy)	3.15 ± 0.81	3.14 ± 0.82	3.03 ± 0.85	3.15 ± 0.67	0.968	0.085
Heart V_{10} (%)	34.70 ± 14.19	35.25 ± 14.55	30.63 ± 12.12	27.34 ± 12.44	0.333	1.160
Heart V_{20} (%)	14.72 ± 7.37	13.55 ± 6.62	30.63 ± 12.12	27.34 ± 12.44	0.000	11.345
Heart V_{30} (%)	7.15 ± 4.86	6.19 ± 3.86	5.03 ± 3.73	6.19 ± 4.84	0.617	0.601
Heart D_{mean} (Gy)	8.72 ± 2.40	8.46 ± 2.22	7.77 ± 1.87	7.58 ± 2.24	0.433	0.929
Cord D_{max} (Gy)	4.41 ± 1.51	3.40 ± 1.75	3.61 ± 2.35	3.70 ± 1.95	0.504	0.791
Contralateral breast V_5 (%)	10.16 ± 8.95	12.43 ± 6.66	11.41 ± 7.06	11.09 ± 8.90	0.890	0.209
Contralateral breast D_{max} (Gy)	6.67 ± 0.81	7.46 ± 1.18	6.95 ± 1.03	6.22 ± 0.68	0.006	4.543
Contralateral breast D_{mean} (Gy)	2.59 ± 0.51	2.69 ± 0.48	2.67 ± 0.46	2.68 ± 0.48	0.935	0.141

Discussion

In our study, optimization based on the biological function increased the D_{mean} of the target. The D_{max} of the target was also increased, which further reduced the uniformity of the target. No significant differences in target CI were observed among the four groups. The biological function was more sensitive to the cold spot in calculating the dose of the target but was not sensitive enough to the hot spot. Therefore, it was not possible to control the hot spot more effectively while increasing the cold spot dose, which increased the D_{max} and D_{mean} and reduced the uniformity of the target. In addition, the MU in the BF group was significantly lower than those of the PF and PF + BF groups, which significantly improved the efficiency of treatment delivery. This advantage is more applicable to clinical work in most radiotherapy departments in China [15].

For OARs, biological function significantly reduced the exposure dose to the ipsilateral lung, showing its absolute advantage in protecting normal lung, while physical function reduced the D_{max} of the contralateral breast. In addition, the relationships between the various dose-volume parameters of the heart, LAD, and spinal cord and biological and physical functions were not obvious. One explanation may be the presence of a dynamic dose balance in the dose distribution. When the dose of the ipsilateral lung was limited, the dose curve would be shifted to the adjacent normal tissues such as the heart or contralateral lung. Second, the spinal cord was away from the target and most of the exposure came from scattering. Therefore, the differences among the four groups were not enough to demonstrate the advantages of biological and physical functions. In addition, LAD had strong individual variability, with the differences in LAD irradiated dose among the four groups greatly affected by its relative anatomical position to the target.

In short, biological function showed a clear advantage in increasing the target dose and decreasing the ipsilateral lung dose and played a positive role in improving TCP and reducing NTCP. The hypofractionation radiotherapy model is becoming increasingly prevalent and the role of biological optimization cannot be ignored. However, this study had several limitations. The relevant biological parameters used in the study were obtained from extensive early clinical experience that requires renewal to further the potential advantages of biological functions in planning.

Conflicts of interest

The authors indicated no potential conflicts of interest.

References

1. Senthilkumar K, Maria Das KJ, Balasubramanian K, *et al*. Estimation of the effects of normal tissue sparing using equivalent uniform dose-based optimization. J Med Phys, 2016, 41: 123–128.
2. Janssen S, Glanzmann C, Lang S, *et al*. Hypofractionated radiotherapy for breast cancer acceleration of the START a treatment regime: intermediate tolerance and efficacy. Radiat Oncol, 2014, 9: 165.
3. Haviland JS, Mannino M, Griffin C, *et al*. Late normal tissue effects in the arm and shoulder following lymphatic radiotherapy: Results from the UK START (Standardisation of Breast Radiotherapy) trials. Radiother Oncol, 2018, 126: 155–162.
4. Chatterjee S, Arunsingh M, Agrawal S, *et al*. Outcomes following a moderately hypofractionated adjuvant radiation (START B type) schedule for breast cancer in an unscreened non-Caucasian population. Clin Oncol (R Coll Radiol), 2016, 28: e165–e172.
5. START Trialists' Group, Bentzen SM, Agrawal RK, *et al*. The UK Standardisation of Breast Radiotherapy (START) trials B of radiotherapy hypofractionation for treatment of early breast cancer: a randomised trial. Lancet, 2008, 371: 1098–1107.
6. Haviland JS, Owen JR, Dewar JA, *et al*. The UK Standardisation of Breast Radiotherapy (START) trials of radiotherapy hypofractionation for treatment of early breast cancer: 10-year follow-up results of two randomised controlled trials. Lancet Oncol, 2013, 14: 1086–1094.
7. Niemierko A. Reporting and analyzing dose distributions: A concept of equivalent uniform dose. Med Phys, 1997, 24: 103–110.
8. Thieke C, Bortfeld T, Niemierko A, *et al*. From physical dose constraints to equivalent uniform dose constraints in inverse radiotherapy planning. Med Phys, 2003, 30: 2332–2339.
9. Wu QW, Mohan R, Niemierko A, *et al*. Optimization of intensity-modulated radiotherapy plans based on the equivalent uniform dose. Int J Radiat Oncol Biol Phys, 2002, 52: 224–235.
10. Hu HQ, Zhang HW, Qiu XP. Optimization results of biological equivalent uniform dose in intensity modulated radiotherapy. Chin J Med Physics, 2016, 33: 190–194.
11. Wang C, Gu JL, Deng QH, *et al*. Clinical value of lung equivalent uniform dose in predicting VMAT-induced radiation pneumonitis. Chin J Radiat Oncol (Chinese), 2017, 26: 749–753.
12. Bentzen SM, Tucker SL. Quantifying the position and steepness of radiation dose-response curves. Int J Radiat Biol, 1997, 71: 531–542.
13. Yarnold J, Ashton A, Bliss J, *et al*. Fractionation sensitivity and dose response of late adverse effects in the breast after radiotherapy for early breast cancer: long-term results of a randomised trial. Radiother Oncol, 2005, 75: 9–17.
14. International Commission on Radiation Units and Measurements. Report 83: prescribing, recording and reporting photon-beam intensity-modulated radiation therapy (IMRT). J ICRU, 2010, 10: 1–106.
15. Lang JY, Wang P, Wu DK, *et al*. An investigation of the basic situation of radiotherapy in the mainland of China in 2015. Chin J Radiat Oncol (Chinese), 2016, 25: 541–545.

DOI 10.1007/s10330-020-0404-4
Cite this article as: Shao Y, Wang YD, Zhang FL, *et al*. Application of biological optimization of hypofractionated radiotherapy post conservative surgery for breast cancer. Oncol Transl Med, 2020, 6: 93–97.

Oncology and Translational Medicine
DOI 10.1007/s10330-019-0341-1

June 2020, Vol. 6, No. 3, P98–P102

ORIGINAL ARTICLE

The efficacy and safety of thalidomide for treating metastatic breast cancer: a systematic review

Xin Wang [1, 2], Yingying Xie [1] (Co-first author), Guanjun Jing [1], Fang Yu [1], Yinghong Ren [1] (✉)

[1] Department of Oncology, Shangluo Central Hospital, Shangluo 726000, China
[2] Department of Medical Oncology, The First Affiliated Hospital of Xi'an Jiaotong University, Xi'an 710061, China

Abstract

Objective This systematic review was conducted to investigate the efficacy and safety of thalidomide in metastatic breast cancer (MBC).

Methods Based on pre-defined inclusion and exclusion criteria, data were independently collected from different databases by three investigators. Overall, three studies were included.

Results The included studies indicated that no patient achieved a partial or complete response from different thalidomide dose levels. Thalidomide was well-tolerated at doses of 100 mg, 200 mg, and 400 mg. In all three studies, common side effects included constipation, somnolence, fatigue, peripheral neuropathy, and dry mouth. Circulating angiogenic factors were not significantly correlated with disease progression.

Conclusion The available evidence indicates that single-agent thalidomide has little or no activity in patients with MBC.

Received: 14 March 2019
Revised: 4 January 2020
Accepted: 12 March 2020

Key words: thalidomide; metastatic breast cancer (MBC); vascular endothelial growth factor (VEGF); tumor necrosis factor-α (TNF-α)

In the late 1950s, thalidomide was synthesized as a non-addictive, non-barbiturate sedative by a German pharmaceutical company. Later, it was discovered that thalidomide was an effective antiemetic and was used to control the symptoms of nausea and vomiting in pregnant women. In 1961, thalidomide was confirmed as the cause of the largest man-made medical disaster in history, with an estimated 10 000 children in 46 countries born with birth defects. Subsequently, thalidomide was withdrawn from the market in most countries. Over the next few decades, its immunomodulatory and antiangiogenic functions were revealed, resulting in novel therapeutic indications. In 1965, Jacob Sheskin serendipitously discovered that its immunomodulatory effects can be used to treat erythema nodosum leprosum (ENL) [1]. In 1994, Robert J. D'Amato [2] and colleagues discovered that orally administered thalidomide inhibits angiogenesis induced by basic fibroblast growth factor (bFGF) in a rabbit corneal micropocket assay. Based on these mechanisms, thalidomide was found to be highly effective in multiple myeloma treatment [3]. Currently, thalidomide is being evaluated for its efficacy in treating solid tumors, such as prostate cancer, glioblastoma, and neck squamous cell carcinoma [4].

Breast cancer is the most common cancer among females worldwide. With early tumor diagnosis, the five-year survival rate is up to 99%. Moreover, several patients remain disease-free throughout their lifetime [5]. However, breast cancer continues to cause more than 0.5 million deaths annually, with over 90% of deaths attributed to metastasis [6]. When cancer cells exit the primary site and spread to various organs, they must undergo several sequential steps. To achieve each step, cancer cells encounter multiple natural barriers, challenging the defined organization and established homeostasis of target organs. Abnormal tumor vessels demonstrate reduced perivascular cell (PVC) coverage, endothelial cell (EC) dissociation, and excess tumor vessel permeability, presenting opportunities for cells to metastasize [7]. In neoplasms, thalidomide exerts anti-inflammatory, anti-proliferative, and antiangiogenic activities [8]. A preclinical experiment utilizing the 4T1 breast cancer cell line has suggested that thalidomide reduces tumor volume and metastasis. The levels of two

✉ Correspondence to: Yinghong Ren. Email: 452131257@qq.com

cytokines, vascular endothelial growth factor (VEGF) and tumor necrosis factor-α (TNF-α) decrease in thalidomide-treated tumor samples when compared with the control group [9]. Currently, thalidomide is tentatively used to treat some cancers, including breast cancer [10–12].

To date, no systematic review has investigated the efficacy and safety of thalidomide monotherapy for treating metastatic breast cancer (MBC). Consequently, we performed a systematic review to gain a perspective on thalidomide use for MBC treatment.

Materials and methods

Search strategy

PubMed, Biomedical Central, Google Scholar, and Cochrane databases were searched using combinations of the following terms: metastatic breast cancer/metastatic breast carcinoma, thalidomide. PubMed – metastatic breast cancer AND thalidomide (limited to English), metastatic breast carcinoma AND thalidomide (limited to English); Biomedical Central – metastatic breast cancer AND thalidomide; Google Scholar – metastatic breast cancer AND thalidomide; Cochrane – metastatic breast cancer AND thalidomide. The search was performed on November 3, 2015. To identify other potentially relevant studies, reference lists from the retrieved studies were searched manually where appropriate.

Selection

Studies were included in the systemic review if they used single-agent thalidomide to treat breast cancer. Studies were excluded if they focused on other stages of breast cancer or failed to analyze efficacy or toxicity.

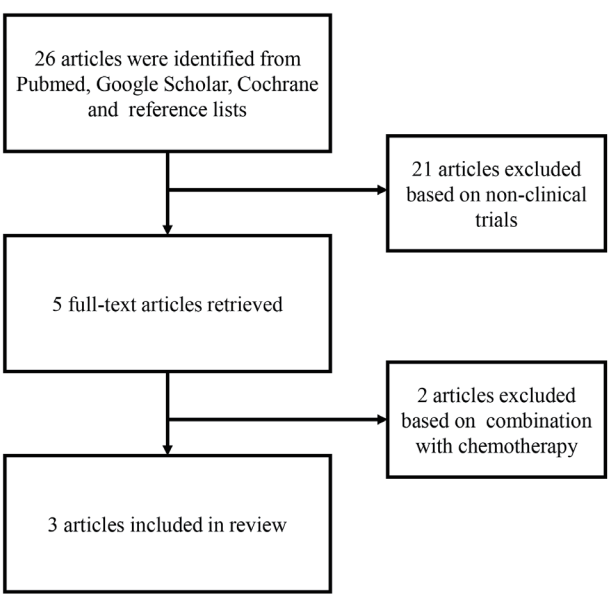

Fig. 1 Flow chart of literature identification and selection process

Data extraction

Data from eligible studies were extracted by two independent reviewers (S.Y.W. and Z.X.M.). Any disagreement was resolved by consulting a third reviewer (Y.J.). The following data were extracted from studies that met the eligibility criteria: author details, publication year, study design, therapeutic regimens, number of patients, patient age, objective response, stable disease, progressive disease, and toxicity response. VEGF, bFGF, and TNF-α levels in patient sera were collected.

Outcome measurement

The primary outcome was the objective response or stable disease with continued treatment until progression. Additionally, toxicity data were summarized. During treatment, serum concentrations of bFGF, TNF-α, and VEGF were measured.

Results

Study selection

In total, 26 articles were identified by searching databases (Fig. 1). After removing 21 non-clinical trials, the full-text of the remaining 5 studies were reviewed, and 2 studies were excluded as thalidomide was combined with chemotherapy. Finally, three studies met the pre-defined criteria and were included in this systematic review.

Study characteristics

The study characteristics and patient clinical data are shown in Table 1. Of the three studies, one was randomly designed, while the others were observational studies. In the study performed by Baidas *et al* [10], 28 patients were randomized based on two thalidomide doses. Overall, 14 patients received a low dose (200 mg/d), and 14 received high-dose (800 mg/d) therapy. Every 2 weeks, an escalation of 200 mg was permitted in the 800 mg/d arm, in patients with no toxicity up to a maximum of 1200 mg/d. In the study undertaken by Eisen *et al* [11], 12 patients with breast cancer were prescribed 100 mg oral thalidomide every night. In the study of Morabito *et al* [12], thalidomide was orally administered at a fixed daily dose of 400 mg for at least 8 weeks. In all three studies, treatment continued until evidence of disease progression or unacceptable toxicity was encountered, or in case the patient wished to discontinue treatment for any reason.

Survival

The prognosis is summarized in Table 2. Based on the investigated thalidomide doses, no patient achieved a partial or complete response. Baidas *et al* reported that

Table 1 Patient characteristics

Characteristic	100-mg daily dose level (*n* = 12)	200-mg daily dose level (*n* = 14)	400-mg daily dose level (*n* = 12)	800-mg daily dose level (*n* = 14)
Age (years)				
30–40	N/A	1	Median 53.5	3
41–50	N/A	7	Range 40–71	2
51–60	N/A	5		4
61–70	N/A	0		4
71–85	N/A	1		1
Prior chemotherapy regimens				
0 or1	N/A	2	N/A	2
2 or 3	N/A	12	9	12
≥ 4	N/A	N/A	3	N/A
High-dose chemotherapy with PBSC support	N/A	3	N/A	2
No. of hormonal therapy courses				
0 or 1	N/A	7	N/A	5
2–4	N/A	7	N/A	9
Site of disease				
Bone only	N/A	1	1	0
Lymph node only	N/A	3	N/A	1
Liver	N/A	1	Viscera (11)	1
Chest	N/A	1	N/A	0
Number of metastatic sites				
1	N/A		1	12
2	N/A	8 (2–4 sites)	4	N/A
3	N/A		6	N/A
≥ 4	N/A		1	N/A
Hormone				
Positive	N/A	N/A	8	N/A
Negative	N/A	N/A	4	N/A

Note: N/A: not applicable

Table 2 Efficacy of thalidomide for inducing remission

Study	Study design	No. of patients	Dose	Rx route	CR + PR	SD	PD
Baidas SM 2000 [10]	RCT	14	200-mg	Po	0	0	13/14
		14	800-mg	Po	0	0	13/14
Eisen T 2000 [11]	Observational study	12	100-mg	Po	0	0	12
Morabito A 2005 [12]	Observational study	12	400-mg	Po	0	0	12

Note: CR, complete response; PR, partial response; SD, stable disease; PD, progressive disease

two patients receiving the 200-mg dose demonstrated disease stability at 8 weeks [10]. The first patient presented a 43% reduction in hilar size and mediastinal lymphadenopathy (site of measurable disease) at 8 weeks. However, at 16 weeks, the disease had progressed, and the patient was excluded from further participation. This patient had previously received adjuvant chemotherapy with cyclophosphamide and doxorubicin, followed by paclitaxel, and then vinorelbine for metastatic disease. The second patient presented a relatively indolent chest-wall disease, progressing slowly with no treatment over the 20 months preceding thalidomide therapy. At the 8-week staging, the disease had stabilized, but the patient was excluded from further participation at week 11 due to grade 3 peripheral neuropathy. At the 200-mg dose level, one patient was removed from the study at week 2 owing to disease progression. At the 400-mg dose level, the time to disease progression did not exceed 10 weeks. At the 800-mg dose level, the time to progression was within 8 weeks. Morabito *et al* reported that the median time to progression was 8 weeks (range, 4–10 weeks) [12]. The median overall survival was 16 weeks (range, 8–54 weeks).

Table 3 Adverse events with thalidomide use

Adverse effect	100-mg daily dose level (*n* = 12)	200-mg daily dose level (*n* = 14)	400-mg daily dose level (*n* = 12)	800-mg daily dose level (*n* = 14)	% of total patients
Constipation	N/A	3 (21%)	7 (58.3%)	10 (71%)	20 (38.4%)
Somnolence	N/A	4 (29%)	7 (58.3%)	8 (57%)	19 (36.5%)
Fatigue	N/A	6 (43%)	N/A	6 (43%)	12 (23.0%)
Peripheral neuropathy	N/A	5 (36%)	N/A	4 (29%)	9 (17.3%)
Dizziness and instability	N/A	2 (14%)	N/A	4 (29%)	6 (11.5%)
Dry mouth	N/A	2 (14%)	N/A	6 (43%)	8 (15.3%)
Skin rash	N/A	1 (7%)	N/A	2 (14%)	3 (5.7%)
Nausea	N/A	0 (0%)	N/A	2 (14%)	2 (3.8%)
Anorexia	N/A	1 (7%)	N/A	1 (7%)	2 (3.8%)
Arrhythmia	N/A	1 (7%)	N/A	0 (0%)	1 (3.8%)
Neutropenia	N/A	1 (7%)	N/A	1 (7%)	2 (3.8%)
Headaches	N/A	1 (7%)	N/A	1 (7%)	2 (3.8%)
Hypotension	N/A	0 (0%)	N/A	1 (7%)	1 (1.9%)
Asthenia	N/A	N/A	4 (33.3%)	N/A	4 (7.6%)

Note: N/A: not applicable

Side effects

In the three studies, all patients were evaluated for toxic effects (Table 3). Thalidomide was well-tolerated at doses of 100 mg, 200 mg, and 400 mg. At the 800-mg dose level, the main side effect was dose-limiting toxicity that required dose reduction in seven patients. In all studies, the most common side effects were constipation and somnolence. In Eisen's study, the precise frequency of adverse events in patients with MBC could not be confirmed [11]. One patient receiving the 200 mg dose was removed because of grade 3 neurotoxicity (peripheral neuropathy). At the 400-mg dose, four patients experienced mild asthenia. Moreover, five serious adverse events were reported in Baidas' study [10]. Furthermore, two patients receiving the 200-mg dose, as well as one administering 800 mg, demonstrated disease progression. Two patients continued treatment with no similar episodes. Of these patients, one receiving the 200-mg dose developed dizziness and palpitations, and the other receiving the 800-mg dose experienced vomiting and headaches necessitating intravenous hydration.

Circulating angiogenic markers

In most patients, circulating angiogenic growth factor levels were detected at baseline. Baidas *et al* reported that baseline and altered TNF-α levels were significantly increased [10]. Additionally, bFGF and VEGF seemed random in a single patient who experienced a near-partial response; however, this patient experienced decreasing serial TNF-α levels from baseline to each time point. Following serial measurements, Eisen *et al* simultaneously observed that rising VEGF levels were associated with disease progression in 6 of 11 patients [11].

Discussion

In this systematic review, we analyzed the efficacy and safety of thalidomide in patients with progressive MBC. In total, 3 studies involving 52 patients were included. As a single agent, thalidomide demonstrated no efficacy in the different dose arms. At the 200-mg dose level, two patients demonstrated stable disease at 8 weeks; however, one patient's improvement was short-lived, and the other case experienced tumor stability at 8 weeks, probably due to the indolent disease history rather than thalidomide therapy.

Based on the negative results of these three studies, the non-hematologic toxicities were mild. Constipation, somnolence, fatigue, peripheral neuropathy, and dry mouth were common. At the 200-mg and 800-mg doses, apart from one patient with grade 3 neuropathy at 200 mg and seven patients with moderate somnolence at 800 mg, no other symptoms required dose modification. Based on observed results, the main side effect was somnolence (dose-limiting toxicity), necessitating dose reduction in the high-dose arm. Thalidomide was well-tolerated at doses of 100 mg and 400 mg. As an antiangiogenic agent, thalidomide can potentially modulate the tumor microenvironment and improve immunotherapy, depending on the optimal dose [13]. In mouse models, thalidomide, at a low concentration, stimulates vessel maturation and increases the cytotoxic agent delivery, increasing survival in the animals [14–16]. In the future, we need to explore the optimal doses of thalidomide combined with chemotherapy, radiotherapy, or immunotherapy. In patients with MBC, thalidomide may be considered a relatively safe agent.

In Colleoni and Eisen's study, baseline levels of

circulating angiogenic growth factors were determined in nearly all patients [11, 19]. No clear relationship was observed between the absolute level of VEGF and tumor response. Notably, the proportion of patients with elevated TNF-α levels was significantly greater, and these TNF-α levels decreased significantly following thalidomide therapy. This may be attributed to the progression of breast cancer. Eisen's study demonstrated increased VEGF levels in six patients with progressive disease [11]. Reportedly, thalidomide inhibits proinflammatory TNF-α production, as well as the effects of bFGF and VEGF on tumor growth in animal models [17–18]; however, TNF-α, VEGF, and bFGF levels may be of limited value in selecting patients for thalidomide therapy or monitoring their therapeutic response. In future studies, we plan to increase the number of samples and/or explore novel biomarkers that may be more reliable.

Here, we systematically reviewed the current literature to compare the efficacy and safety of single-dose thalidomide for MBC therapy. Notably, available evidence indicates no potential survival advantage from thalidomide monotherapy. In two phase II studies evaluating chemotherapy in combination with thalidomide, Colleoni *et al* have suggested that adding thalidomide failed to benefit patients with MBC [3, 19]. However, these results do not preclude the efficacy of thalidomide in other settings, such as in patients with other malignancies [20]. Moreover, they do not preclude the drug's possible activity when combined with other classically active agents, such as hormone therapy or immunomodulators. In conclusion, further well-designed and prospective studies need to be undertaken.

Conflicts of interest

The authors indicated no potential conflicts of interest.

References

1. Sheskin J. Thalidomide in the treatment of lepra reactions. Clin Pharmacol Ther, 1965, 6: 303–306.
2. D'Amato RJ, Loughnan MS, Flynn E, *et al*. Thalidomide is an inhibitor of angiogenesis. Proc Natl Acad Sci USA, 1994, 91: 4082–4085.
3. Singhal S, Mehta J, Desikan R, *et al*. Antitumor activity of thalidomide in refractory multiple myeloma. N Engl J Med, 1999, 341: 1565–1571.
4. Eleutherakis-Papaiakovou V, Bamias A, Dimopoulos MA. Thalidomide in cancer medicine. Ann Oncol, 2004, 15: 1151–1160.
5. Miller AB, Wall C, Baines CJ, *et al*. Twenty five year follow-up for breast cancer incidence and mortality of the Canadian National Breast Screening Study: randomised screening trial. BMJ, 2014, 348: g366.
6. Subramanian A, Manigandan A, Sivashankari PR, *et al*. Development of nanotheranostics against metastatic breast cancer – A focus on the biology & mechanistic approaches. Biotechnol Adv, 2015, 33: 1897–1911.
7. Goel S, Wong AH, Jain RK. Vascular normalization as a therapeutic strategy for malignant and nonmalignant disease. Cold Spring Harb Perspect Med, 2012, 2: a006486.
8. Zhou S, Wang F, Hsieh TC, *et al*. Thalidomide – a notorious sedative to a wonder anticancer drug. Curr Med Chem, 2013, 20: 4102–4108.
9. Maria de Souza C, Fonseca de Carvalho L, da Silva Vieira T, *et al*. Thalidomide attenuates mammary cancer associated-inflammation, angiogenesis and tumor growth in mice. Biomed Pharmacother, 2012, 66: 491–498.
10. Baidas SM, Winer EP, Fleming GF, *et al*. Phase II evaluation of thalidomide in patients with metastatic breast cancer. J Clin Oncol, 2000, 18: 2710–2717.
11. Eisen T, Boshoff C, Mak I, *et al*. Continuous low dose thalidomide: a phase II study in advanced melanoma, renal cell, ovarian and breast cancer. Br J Cancer, 2000, 82: 812–817.
12. Morabito A, Carillio G, Longo R, *et al*. Thalidomide is inactive in heavily pretreated patients with metastatic breast cancer. Cancer J, 2005, 11: 248–251.
13. Huang Y, Yuan J, Righi E, *et al*. Vascular normalizing doses of antiangiogenic treatment reprogram the immunosuppressive tumor microenvironment and enhance immunotherapy. Proc Natl Acad Sci USA, 2012, 109: 17561–17566.
14. Lebrin F, Srun S, Raymond K, *et al*. Thalidomide stimulates vessel maturation and reduces epistaxis in individuals with hereditary hemorrhagic telangiectasia. Nat Med, 2010, 16: 420–428.
15. Segers J, Fazio VD, Ansiaux R, *et al*. Potentiation of cyclophosphamide chemotherapy using the anti-angiogenic drug thalidomide: Importance of optimal scheduling to exploit the "normalization" window of the tumor vasculature. Cancer Lett, 2006, 244: 129–135.
16. De Souza CM, Araújo e Silva AC, De Jesus Ferraciolli C, *et al*. Combination therapy with carboplatin and thalidomide suppresses tumor growth and metastasis in 4T1 murine breast cancer model. Biomed Pharmacother, 2014, 68: 51–57.
17. Verheul HM, Panigrahy D, Yuan J, *et al*. Combination oral antiangiogenic therapy with thalidomide and sulindac inhibits tumour growth in rabbits. Br J Cancer, 1999, 79: 114–118.
18. Muller GW, Corral LG, Shire MG, *et al*. Structural modifications of thalidomide produce analogs with enhanced tumor necrosis factor inhibitory activity. J Med Chem, 1996, 39: 3238–3240.
19. Colleoni M, Orlando L, Sanna G, *et al*. Metronomic low-dose oral cyclophosphamide and methotrexate plus or minus thalidomide in metastatic breast cancer: antitumor activity and biological effects. Ann Oncol, 2006, 17: 232–238.
20. Ge YN, Zheng ZD, Liu ZZ, *et al*. Effect of etoposide plus thalidomide as maintenance therapy on progression-free survival of elderly patients with advanced non-small cell lung cancer. Oncol Transl Med, 2017, 3: 103–107.

DOI 10.1007/s10330-019-0341-1
Cite this article as: Wang X, Xie YY, Jing GJ, *et al*. The efficacy and safety of thalidomide for treating metastatic breast cancer: a systematic review. Oncol Transl Med, 2020, 6: 98–102.

Oncology and Translational Medicine
DOI 10.1007/s10330-020-0402-2

June 2020, Vol. 6, No. 3, P103–P108

ORIGINAL ARTICLE

Effect of miR-375 on non-small cell lung carcinoma invasion, migration, and proliferation through the CIP2A pathway

Junyu Wu[1], Weijun Yuan[2], Yuhuan Wang[2], Xiaodong Zhao[1] (✉)

[1] Department of Emergency, The Fourth Medical Center of General Hospital of Chinese People's Liberation Army, Beijing 100037, China
[2] Department of Special Medicine, School of Basic Medical College, Qingdao University, Qingdao 266021, China

Abstract

Objective The aim of this study was to study the effect of miR-375 on non-small cell lung carcinoma (NSCLC) invasion, migration, and proliferation through the CIP2A pathway.

Methods We constructed a stable over-expressing cell line with lentivirus as the experimental group (Lv-miR-375) and transfected the empty vector as the negative control group (Lv-NC). The expression level of miR-375 was detected using real-time fluorescence quantitative PCR (qRT-PCR).Western blots were used to detect the expression levels of cancerous inhibitor of PP2A (CIP2A), MYC, protein kinase B (AKT) and p-AKT in Lv-NC- and Lv-miR-375-transfected cells. Transwell assays were conducted to detect the cell invasion and metastasis ability, and the cell counting kit-8 (CCK8) was used to detect cell proliferation.

Results qRT-PCR showed that miR-375 was overexpressed in NSCLC. Compared to the Lv-NC-transfected cells, the western blot results showed that CIP2A, MYC and p-AKT were highly expressed in Lv-miR-375-transfected cells. Transwell assays showed that the invasion and migration ability of Lv-miR-375-transfected A549 cells was significantly higher than that of Lv-NC-transfected cells. CCK8 experiments showed that compared to Lv-NC-transfected cells, the cell proliferation ability of the Lv-miR-375-transfected cells increased.

Conclusion MiR-375 could promote the invasion, migration, and proliferation of NSCLC A549 cells via the CIP2A pathway. MiR-375 is expected to become a new target for the treatment of NSCLC, and may become an important biomarker for the diagnosis, prognosis, and treatment of the disease.

Received: 16 January 2020
Revised: 4 March 2020
Accepted: 20 April 2020

Key words: miR-375; invasion; migration; non-small cell lung cancer (NSCLC); CIP2A

Lung cancer is one of the malignant tumors with the fastest increase in morbidity and mortality and the greatest threat to people's health and life. Worldwide, lung cancer is the leading cause of cancer death in men and the second leading cause of cancer deaths in women [1]. Lung cancer is divided into two major groups, small cell lung cancer (SCLC) and non-small cell lung cancer (NSCLC) [2]. SCLC accounts for approximately 20% of lung cancers. It has a high degree of malignancy and early metastasis, and is sensitive to chemotherapy and radiotherapy. The initial remission rate is high, but it is prone to secondary drug resistance and relapse. Chemotherapy is the mainstay. NSCLC includes three major histological subtypes, lung squamous cell carcinoma (SCC), lung adenocarcinoma (ADC), and large cell lung cancer (LCLC), accounting for approximately 80% of lung cancers. Cell division is slower, and the diffusion shift is relatively late [3]. Nevertheless, while current research on the biological characteristics of different histological subtypes of NSCLC is expanding, its basic molecular mechanism is not yet clear. For example, smoking is more risky for SCC than ADC [4].

Micro-RNA is an endogenous small RNA with a length of approximately 19–25 nucleotides. As a short non-coding RNA, its main function is to regulate the

✉ Correspondence to: Xiaodong Zhao. Email: zxd63715@126.com

expression level of mRNA. miRNAs can be used as proto-oncogenes or tumor suppressors, and participate in various processes including proliferation, apoptosis, metabolism, and differentiation of cells through targeted binding to different transcripts [5]. miRNAs are expressed in specific tissue and developmental stages under normal physiological conditions, but abnormal expression of miRNAs can lead to a series of pathological states, such as tumorigenesis and metastasis [6–7]. miRNA regulates the function of tumor cells by regulating the expression of functional proteins. For example, miR-206 promotes breast cancer proliferation by inhibiting estrogen receptor alpha (ERα) while miR-34a downregulates E2 factor transcription factor 2 (E2F2) expression to regulate the cell cycle and apoptosis [8–9].

CIP2A, as an oncogenic protein during the malignant transformation and progression of cancer cells, has been shown to have a certain relationship with the efficacy of many drugs in cancer treatment. Oncoprotein CIP2A, also known as KIAA1524 or P90, was named in 2007 and is a cancerous inhibitor of PP2A due to its effect on cancer cells. The stability of PP2A and MYC is controlled to form a "carcinogenic connection" [10].

In this study, we found that miR-375 regulated the expression of downstream protein kinase B (AKT), MYC, p-AKT and other related proteins through the CIP2A/PP2A signaling pathway, inhibiting the cancer phenotype of lung cancer, and affecting cell invasion, proliferation, apoptosis, and the cell morphology process. We found that the CIP2A gene is a direct binding target of miR-375. Thus, it has become a topic of great interest to explore whether and how miR-375 regulates ADC cells through the CIP2A signaling pathway. By up-regulating miR-375 in a lentivirus-transfected A549 cell line, we found that a series of phenotypes, including cell invasion, proliferation, and apoptosis were changed, and that CIP2A and its downstream signaling proteins were also changed.

Material and methods

Cell culture and transfection

The human lung adenocarcinoma cell line, A549 (Jikai Gene Company), was cultured in Roswell Park Memorial Institute (RPMI) 1640 (Solarbio Company) medium containing 10% fetal bovine serum (FBS, Solarbio Company), 100 U/mL penicillin, and 100 U/mL streptomycin at 37 °C under 5% CO_2. After the cells were grown to logarithmic growth phase, they were incubated at 37 °C for 10 h according to the instructions of the transfection kit. They were then transfected with a multiplicity of infection of 25 of miR-375-expressing lentivirus (Lv-miR-375) (Jikai Gene Company) and control lentivirus (Lv-NC) (Jikai Gene Company); then, the transfected A549 cells were stained.

RNA extraction and real-time fluorescence quantitative PCR (qRT-PCR)

After extraction of total cellular RNA with RNAIso plus, the reverse transcription reaction was performed using the PrimeScript RT reagent kit with gDNA Eraser (Perfect Real Time). The reverse transcription primer for miR-375 was 5′-GTCGTATCCAGTGCAGGGTCC GAGGTATTCGCACTGGATACGACACTGCC-3′. The RT-PCR primer sequences were: upstream primer 5′-GGACAGCAGGCACAGACA-3′, and downstream primer 5′-CAGTGCAGGGTCCGAGGT-3′. The PCR primers for the *CIP2A* sequence were: upstream primer 5′-ATGCAAACTTGCTGCTGATG-3′, and downstream primer 5′-ATCAAACGTGGGTCCTGAAG-3′. The U6 small nuclear RNA was used as an endogenous reference for miRNA and *β-ACTIN* was used as an endogenous reference for the target gene mRNA. The reaction was performed using SYBR green, with the following conditions: denaturation at 95°C for 10 min, followed by 40 cycles of denaturation at 95°C for 5 s, annealing at 60°C for 34 s, and fluorescence detection at 74°C for 3 s. The difference between the two was compared with the $2^{-\Delta\Delta Ct}$ values, and 3 replicates were used for each group of experiments.

Western Blot

A western blot assay was used to detect protein expression levels. The total protein lysate was extracted using instruction manual and stored at –80°C for later use. According to the kit instructions, the protein concentration was determined using a bicinchoninic acid assay, diluted, and mixed with 5× loading buffer. Proteins were denatured at 95°C for 10 min, and a 50 μg sample was loaded to separate proteins by electrophoresis. After electrophoresis, proteins were transferred to polyvinylidene difluoride membranes and blocked with 5% skim milk powder in a shaker for 1 h at room temperature. Membrane strips were placed in one of the following primary antibodies and incubated overnight at 4°C: AKT (1:1000, Cell Signaling Technology (CST), USA), p-AKT (1:1000, CST, USA), MYC (1:1000, CST, USA), CIP2A (1:1000, CST, USA), and β-ACTIN (1:3000, CST, USA). Membranes were washed three times with Tris-buffered saline, 0.1% Tween 20 (TBST), 10 min/wash, and incubated with the secondary antibody for 2 h at room temperature. Membranes were washed three times with TBST, 10 min/wash, soaked in enhanced chemiluminescent (ECL) solution, and the strip was placed in the cartridge and exposed in the darkroom. Bands were analyzed using grayscale analysis with Photoshop CS6, and statistics were conducted on the grayscale analysis values.

Transwell Assay

For the invasion test, Matrigel® and serum-free medium were diluted 1:9. The dilution (100 μL) was added to the Transwell chamber and placed in a 37 °C incubator for 4 h. Then, 50,000 cells each of Lv-NC- and Lv-miR-375-transfected cells were added to the Transwell chamber, 20% FBS containing RPMI 1640 was added to the lower chamber, and the Transwell chamber was incubated at 37 °C for 48 h. The chamber was removed from the incubator, the culture solution from the upper chamber was removed, and the cells in the upper chamber were scraped off with a sterile cotton swab. After fixing for 10 min with methanol, cells were stained with crystal violet for 10 min and then photographed. This experiment was repeated three times.

For the migration test, 50,000 cells each of Lv-NC- and Lv-miR-375-transfected cells were added to the Transwell chamber. The experimental procedure was followed by an invasive experiment. This experiment was repeated three times.

Cell Counting Kit-8 (CCK8) assay

To measure cell proliferation, 3000 cells of the Lv-NC- and Lv-miR-375-transfected cells were seeded into 96-well plates, and the CCK8 reagent was added at 24, 48, and 72 h, respectively, and then detected 4 h later. This experiment was repeated three times.

Statistical analysis

GraphPad Prism 5 software was used for statistical analysis. Statistical results are expressed as the mean ± standard deviation. Comparisons among groups for the RT-PCR and western blots were performed using one-way analysis of variance. The test level was $P = 0.05$ and $P < 0.05$ was considered significant. All experiments were repeated three times.

Results

MiR-375 was highly expressed in NSCLC

As shown in Fig. 1a, compared to normal human lung epithelial cells, BEAS-2B, the expression levels of miRNA-375 were significantly upregulated in transfected A549 cells ($P < 0.01$). As shown in Fig. 1b, compared to Lv-NC-transfected cells, the expression of miRNA-375 was significantly increased in Lv-miR-375-transfected cells ($P < 0.01$).

MiR-375 promoted invasion and metastasis of NSCLC

Compared to Lv-NC-transfected cells, the metastasis ability (Fig. 2a and 2c, $P < 0.01$) and invasive ability (Fig. 2b and 2d, $P < 0.01$) of Lv-miR-375-transfected cells was increased. This experiment demonstrated that miR-375 promoted the invasion and metastasis ability of NSCLC.

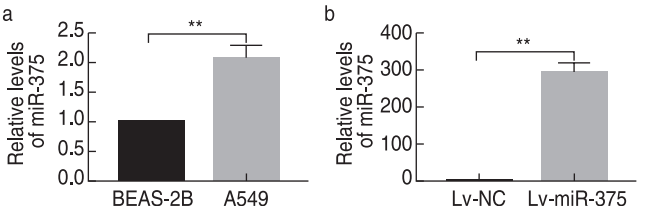

Fig. 1 Expression levels of miR-375 are upregulated in NSCLC. (a) Relative levels of miR-375 in BEAS-2B and A549 cell lines. (b) Relative levels of miR-375 in Lv-NC- and Lv-miR-375-transfected cells. $^{**}P < 0.01$

MiR-375 promoted the proliferation of NSCLC

Compared to Lv-NC-transfected cells, the proliferation ability of cells was increased in Lv-miR-375-transfected cells (Fig. 3; $P < 0.01$). This experiment demonstrated that miR-375 promoted the proliferation ability of NSCLC.

Western blot

Western blot analysis of CIP2A, MYC, AKT, p-AKT and β-ACTIN protein expression in A549 cells after transfection with Lv-NC and Lv-miR-375 demonstrated that miR-375 promoted the expression of CIP2A, p-AKT/AKT and MYC protein levels. Compared to Lv-NC-transfected cells, the expression level of CIP2A (Fig. 4a and 4d, $P < 0.01$), p-AKT/AKT (Fig. 4a and 4b, $P < 0.01$) and MYC (Fig. 4a and 4c, $P < 0.01$) was increased in Lv-miR-375-transfected cells.

Discussion

Since miR-375 was discovered, it has gradually become a hot topic in the field of cancer research. miRNAs can degrade mRNA or inhibit protein translation at the post-transcriptional level through complete or incomplete complementary pairing with the 3′ non-coding region of target mRNAs. In ontogenesis, cell differentiation, and proliferation, it plays an important role in life activities, such as apoptosis. miRNAs bind to complementary sequences in the 3′ untranslated region (UTR) of their target mRNAs and induce mRNA degradation or translational inhibition [11]. Because of these mechanisms, miRNAs can regulate the expression of target genes, so miRNAs can have an anti-tumor role. Genes also play an important role, including those that drive apoptosis, those that inhibit cell proliferation and those that regulate drug efflux mechanisms [12–14]. miRNAs may act as oncogenes or tumor suppressors in the occurrence and development of tumors. By inhibiting the role of tumor suppressor genes or regulating cell apoptosis, and promoting tumorigenesis and development, miRNAs can also act as oncogenes [15–16].

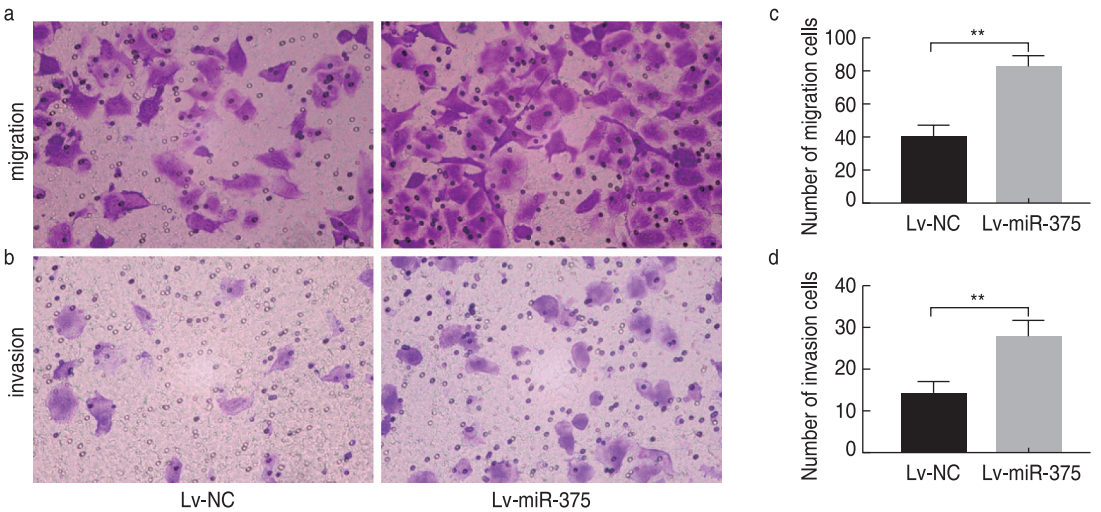

Fig. 2 MiR-375 promotes the invasion and metastasis ability of NSCLC. (a and c): Transwell migration assays in A549 cells after transfection with Lv-NC and Lv-miR-375. (b and d): Transwell invasion assays in A549 cells after transfection with Lv-NC and Lv-miR-375. $^{**}P < 0.01$

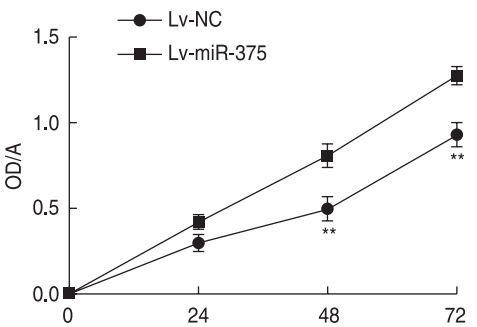

Fig. 3 MiR-375 promotes the proliferation ability of NSCLC. $^{**}P < 0.01$

The cancerous inhibitor of protein phosphatase 2A (CIP2A) is a recently identified human oncoprotein that inhibits c-MYC protein degradation in many cancer cells. CIP2A inhibits the degradation of proto-oncogenes in tumor cells by inhibiting the phosphorylation of the proto-oncogene serine 62 (S62) to regulate the expression of stable proto-oncogene proteins by inhibiting the serine of protein phosphatase 2 (PP2A). With a threonine phosphatase function, CIP2A can activate oncogenic proteins, such as proto-oncogenes (MYC), extracellular signal-regulated kinase (ERK) and AKT. Previous studies have shown that CIP2A is the main molecule that induces apoptosis of bortezomib-induced apoptosis in head and neck squamous cell carcinoma (HNSCC), triple negative breast cancer (TNBC), leukemia cells, and hepatocellular carcinoma (HCC) [17–20]. Recent studies have proposed a comprehensive interrelated CIP2A regulatory network (with an oncogenic correlation) that was established through direct interaction of multiple key cell proteins/transcription factors or CIP2A components of major oncogenic pathways or indirect CIP2A-PP2A completed interactions [21].

Related studies have found that miR-375 can influence tumor proliferation and apoptosis expression [22–24]. Therefore, we suspect that miR-375 may be an important target for the treatment of lung cancer and could improve prognosis. We decided to study miR-375 after consulting

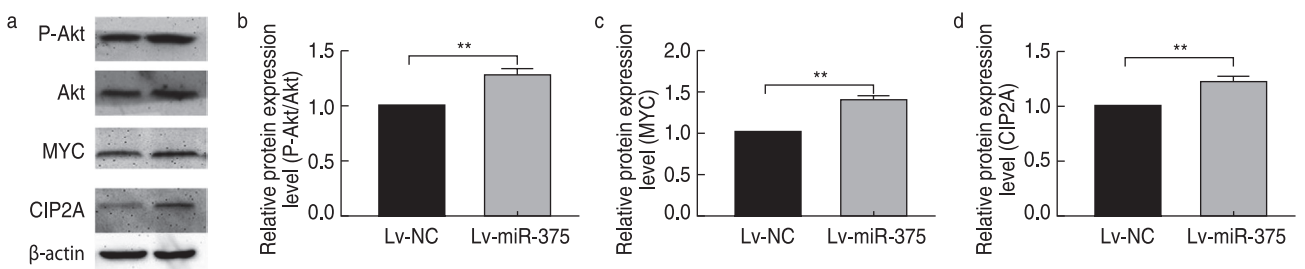

Fig. 4 MiR-375 increases the expression of CIP2A, p-AKT/AKT, and MYC. (a) Western blot assays for CIP2A, p-AKT, AKT, MYC, and β-ACTIN in A549 cells after transfection with Lv-NC and Lv-miR-375; (b) Analysis of p-AKT and AKT western blot results; (c) Analysis of CIP2A western blot results; (d) Analysis of MYC western blot results. $^{**}P < 0.01$

relevant domestic and foreign literature. After screening, miR-375 was highly expressed in the NSCLC A549 cell line. Among all types of lung cancer, NSCLC accounts for approximately 85%, and the 5-year survival rate is 15% [25]. When we up-regulated miR-375 in A549 cells, we found that cell invasion, metastasis, and proliferation were increased, apoptosis was reduced, and CIP2A and MYC were elevated with increasing levels of miR-375. miR-375 could affect lung cancer invasion, proliferation, and apoptosis ability through CIP2A, MYC and the epithelial-to-mesenchymal transition. We identified CIP2A as a novel miR-375 target that was regulated by post-transcriptional control through multiple binding sites on the CIP2A coding region and thus stabilized the oncogenic MYC. However, the specific mechanisms involved in miR-375, its effect on NSCLC, and the many uncertainties in the application of targets to the clinic require further scientific research.

In this experiment, miRNA-375 was over-expressed in the lung cancer cell line A549 by recombinant lentivirus transfection. A quantitative detection of the target protein was performed using western blot analysis. At the same time, Transwell assays were used to test the invasion and migration of cells. The proliferation of cell lines was determined by CCK-8. Compared to Lv-NC-transfected cells, these experiments have confirmed that the ability of cells to invade, metastasize and proliferate was increased in Lv-miR-375-transfected cells. This study further investigated the effect and interaction of miR-375 on the CIP2A pathway in lung cancer A549 cells. Western blot analysis detected the expression of major proteins, including MYC and p-AKT in the CIP2A pathway, and showed that miR-375 could significantly up-regulate MYC and p-AKT protein expression.

Taken together, these results suggested that miR-375 promoted invasion, migration, and proliferation of NSCLC via the CIP2A pathway. Therefore, miR-375 is expected to become a new target for neoplastic diseases and drug treatment. It is also likely to become a very important biomarker for early diagnosis, prognosis, and treatment of diseases.

Conflicts of interest

The authors indicated no potential conflicts of interest.

References

1. Torre LA, Siegel RL, Jemal A. Lung Cancer Statistics. Adv Exp Med Biol, 2016, 893: 1–19.
2. Nishikawa E, Osada H, Okazaki Y, *et al*. miR-375 is activated by ASH1 and inhibits YAP1 in a lineage-dependent manner in lung cancer. Cancer Res, 2011, 71: 6165–6173.
3. Capelletto E, Novello S. Emerging new agents for the management of patients with non-small cell lung cancer. Drugs, 2012, 72: 37–52.
4. Sobue T, Yamamoto S, Hara M, *et al*. Cigarette smoking and subsequent risk of lung cancer by histologic type in middle-aged Japanese men and women: the JPHC study. Int J Cancer, 2002, 99: 245–251.
5. Lewis BP, Shih IH, Jones-Rhoades MW, Bartel DP, Burge CB: Prediction of mammalian microRNA targets. Cell, 2003,115: 787–798.
6. Shore AN, Herschkowitz JI, Rosen JM. Noncoding RNAs involved in mammary gland development and tumorigenesis: there's a long way to go. J Mammary Gland Biol Neoplasia, 2012, 17: 43–58.
7. Ventura A, Jacks T. MicroRNAs and cancer: short RNAs go a long way. Cell, 2009,136: 586–591.
8. Welch C, Chen Y, Stallings RL. MicroRNA-34a functions as a potential tumor suppressor by inducing apoptosis in neuroblastoma cells. Oncogene, 2007, 26: 5017–5022.
9. Adams BD, Furneaux H, White BA. The micro-ribonucleic acid (miRNA) miR-206 targets the human estrogen receptor-alpha (ERalpha) and represses ERalpha messenger RNA and protein expression in breast cancer cell lines. Mol Endocrinol, 2007, 21: 1132–1147.
10. De P, Carlson J, Leyland-Jones B, *et al*. Oncogenic nexus of cancerous inhibitor of protein phosphatase 2A (CIP2A): an oncoprotein with many hands. Oncotarget, 2014, 5: 4581–4602.
11. Engels, BM, Hutvagner, G. Principles and effects of microRNA-mediated post-transcriptional gene regulation. Oncogene, 25: 6163–6169.
12. Yu HW, Cho WC. The emerging role of miRNAs in combined cancer therapy. Expert Opin Biol Ther, 2015, 15: 923–925.
13. Zhao Y, Srivastava D. A developmental view of microRNA function. Trends Biochem Sci, 2007, 32:189–197.
14. Ao X, Nie P, Wu B, *et al*. Decreased expression of microRNA-17 and microRNA-20b promotes breast cancer resistance to taxol therapy by upregulation of NCOA3. Cell Death Dis, 2016, 7: e2463.
15. Jiang Q, Wang Y, Hao Y, *et al*. miR2Disease: a manually curated database for microRNA deregulation in human disease. Nucleic Acids Res, 2009, 37(Database issue): D98–D104.
16. Calin GA, Croce CM. MicroRNA signatures in human cancers. Nat Rev Cancer, 2006, 6: 857–866.
17. Tseng LM, Liu CY, Chan KC, *et al*. CIP2A is a target of Bortezomib in human triple negative breast cancer cells. Breast Cancer Res, 2012, 14: R68.
18. Lin YC, Chen KC, Chen CC, *et al.* CIP2A-mediated Akt activation plays a role in bortezomibinduced apoptosis in head and neck squamous cell carcinoma cells. Oral Oncol, 2012, 48: 585–593.
19. Liu CY, Shiau CW, Kuo HY, *et al*. Cancerous inhibitor of protein phosphatase 2A determines bortezomibinduced apoptosis in leukemia cells. Haematologica, 2013, 98: 729–738.
20. Chen KF, Liu CY, Lin YC, *et al*. CIP2A mediates effect of bortezomib on phospho Akt and apoptosis in hepatocellular carcinoma cells. Oncogene, 2010, 29: 6257–6266.
21. De P, Carlson J, Leyland-Jones B, *et al*. Oncogenic nexus of cancerous inhibitor of protein phosphatase 2A (CIP2A):an oncoprotein with many hands. Oncotarget, 2014, 5: 4581–4602.
22. Chen HY, Liu C, Jiang H, *et al*. Regulatory role of miRNA-375 in expression of BMP15/GDF9 receptors and its effect on proliferation and apoptosis of bovine cumulus cells. Cell Physiol Biochem, 2017, 41: 439–450.
23. Zhang LX, Jin W, Zheng J, *et al*. MicroRNA-375 regulates proliferation and apoptosis of glioma cancer cells by inhibiting CTGF-EGFR signaling pathway. Bratisl Lek Listy, 2018, 119:17–21.
24. Zhou N, Qu Y, Xu C, *et al*. Upregulation of microRNA-375 increases the cisplatin-sensitivity of human gastric cancer cells by regulating

ERBB2. Exp Ther Med, 2016, 11: 625–630.
25. Torre LA, Bray F, Siegel RL, *et al*. Global cancer statistics, 2012. CA Cancer J Clin, 2015, 65: 87–108.

DOI 10.1007/s10330-020-0402-2
Cite this article as: Wu JY, Yuan WJ, Wang YH, *et al*. Effect of miR-375 on non-small cell lung carcinoma invasion, migration, and proliferation through the CIP2A pathway. Oncol Transl Med, 2020, 6: 103–108.

Oncology and Translational Medicine
DOI 10.1007/s10330-020-0408-8
June 2020, Vol. 6, No. 3, P109–P115

ORIGINAL ARTICLE

Prognostic risk model construction and prognostic biomarkers identification in esophageal adenocarcinoma based on immune-related long noncoding RNA*

Kai Qin[1], Yi Cheng[1], Jing Zhang[1], Xianglin Yuan[1], Jianhua Wang[1], Jian Bai[2] (✉)

[1] Department of Oncology, Tongji Hospital, Tongji Medical College, Huazhong University of Science and Technology, Wuhan 430030, China
[2] Department of Obstetrics and Gynecology, Tongji Hospital, Tongji Medical College, Huazhong University of Science and Technology, Wuhan 430030, China

Abstract

Objective The aim of this study was to construct a prognostic model of esophageal adenocarcinoma (EAC) based on immune-related long noncoding RNAs (immune-related lncRNAs) and identify prognostic biomarkers using the Cancer Genome Atlas (TCGA) database.

Methods Whole genomic mRNA expression and clinical data of esophageal adenocarcinoma were obtained from the TCGA database. The software Strawberry Perl, R and R packets were used to identify the immune-related genes and lncRNAs of esophageal adenocarcinoma, and for data processing and analysis. The differentially expressed lncRNAs were detected while comparing esophageal adenocarcinoma and normal tissue samples. The key immune-related lncRNAs were screened using lasso regression analysis and univariate cox regression analysis, and used to construct the prognostic model using multivariate cox regression analysis.

To evaluate the accuracy of the risk prognostic model, all esophageal adenocarcinomas were divided into high-risk and low-risk groups according to the median risk score, after which Kaplan-Meier (K-M) survival curves, operating characteristic (ROC) curve and independent prognostic analysis of clinical traits were created. In addition, statistically significant immune-related lncRNAs and potential prognostic biomarkers were identified using the prognostic model and multifactor cox regression analysis for k-m survival analysis.

Results A total of 1322 differentially expressed immune-related lncRNAs were identified, 28 of which were associated with prognosis via univariate cox regression analysis. In addition, K-M survival analysis showed that the total survival time of the higher risk group was significantly shorter than that of the lower risk group (P = 1.063e−10). The area under the ROC curve of 5-year total survival rate was 0.90. The risk score showed independent prognostic risk for esophageal adenocarcinoma via single factor and multifactorial independent prognostic analyses. In addition, the HR and 95% CI of each key immune-related lncRNA were calculated using multivariate Cox regression. Using k-m survival analysis, we found that 5 out of 12 key significant immune-related lncRNAs had independent prognostic value [AL136115.1 (P = 0.006), AC079684.1 (P = 0.008), AC07916394.1 (P = 0.0386), AC087620.1 (P = 0.041) and MIRLET7BHG (P = 0.044)].

Conclusion The present study successfully constructed a prognostic model of esophageal adenocarcinoma based on the TCGA database, with moderate predictive accuracy. The model consisted of the expression level of 12 immune-related lncRNAs. Furthermore, the study identified one favorable prognostic biomarker, MIRLET7BHG, and four poor prognostic biomarkers (AL136115.1, AC079684.1, AC016394.1, and AC087620.1).

Received: 20 February 2020
Revised: 11 March 2020
Accepted: 25 March 2020

Key words: immune-related Cancer Genome Atlas (lncRNA); prognostic model; prognostic biomarker; esophageal adenocarcinoma (EAC); Cancer Genome Atlas (TCGA) database

✉ Correspondence to: Jian Bai. Email: 26062793@qq.com
* Supported by a grant from the Health Commission of Hubei Province Scientific Research Project (No. WJ2019M118).

Esophageal cancer is one of the most common malignant cancer of digestive tract [1]. In China, esophageal cancer, which is the sixth deadliest cancer worldwide, accounted for 6.25% of all new cases of malignant cancers in 2015, with an estimated 245,700 new cases [2]. The overall survival rate of esophageal cancer is still low and the burden of this malignancy is particularly high in China [2]. It accounts for 20% of the world's esophageal cancer [3]. About 50% of all global deaths from esophageal cancer occur in China [3–4]. Two major histological subtypes, esophageal adenocarcinoma (EAC) and squamous cell carcinoma (ESCC), show significantly different patterns, and the combination of these two types represent the vast majority of esophageal cancer [2]. EAC is the main type in western developed countries [5]. Melina Arnold *et al* predicted a dramatic increase of EAC in high-income countries, surpassing ESCC in the next few years [6]. Cowie A *et al* found that countries such as Japan are beginning to observe rising rates of EAC, likely due to the 'westernization' of their lifestyle [5]. Although there are many risk assessment models of esophageal carcinoma worldwide, most of them are prognostic models of ESCC with some limitations [7]. Therefore, constructing predictive models and prognostic markers of esophageal adenocarcinoma may prove helpful for prognosis judgment and treatment selection.

Long noncoding RNAs (lncRNAs) belong to a class of endogenous RNAs with a length of more than 200 nucleotides, which regulate a variety of malignant tumor phenotypes through epigenetic modification, RNA decay and transcriptional regulation participate in biological processes such as proliferation, differentiation, and invasion of tumor cells [8]. Numerous lncRNAs are abnormally expressed in ESCC (*e.g.* actin filament-associated protein 1-antisense RNA 1 (AFAP1-AS1), metastatic lung adenocarcinoma transcript 1 (MALAT1), hox contraindic intergenic RNA (HOTAIR), taurine upregulated gene 1 (TUG1), etc. These aberrantly expressed lncRNAs play an important role in the occurrence and development of ESCC, possibly promoting or inhibiting cancer development, and therefore, could be potential biomarkers for ESCC prognostic assessment [9–11]. Esophageal adenocarcinoma is the main risk prediction model for esophageal cancer in Europe and Australia. Mostly, the research designs have focused on case-control and cohort studies, and non-genetic prediction variables are used to construct a risk scoring model. To date, there is no risk scoring model constructed with lncRNAs as predictive variables in esophageal adenocarcinoma [7].

Using whole genomic mRNA expression and clinical data from the TCGA database, the present study constructed an immune-related lncRNA prognostic risk model and identified prognostic biomarkers in esophageal adenocarcinoma.

Materials and methods

Acquisition of esophageal adenocarcinoma expression data

Whole genomic mRNA expression and clinical data for esophageal adenocarcinoma were downloaded from the TCGA database (https://portal.gdc.cancer.gov/). The screening conditions were as follows: (1) primary tumor site: esophageal cancer; (2) project: TCGA-ESCA; (3) disease type: adenocarcinoma or adenoma; (4) data category: transcriptome profiling; (5) data type: gene expression quantification; (6) experimental strategy: RNA-Seq; (7) workflow type: HTSeq-fpkm; (8) remaining screening criteria: default or unselected. The dataset downloaded in January 14, 2020 was integrated into a matrix using the Strawberry-Perl software (version 5.30.1.1–64 bits). We obtained the entire messenger RNA (mRNA) spectrum data and the clinical information of the samples (number of patients, survival time, survival status, sex, clinical stages and TNM stage).

Immune-related genes and lncRNA for esophageal adenocarcinoma

The mRNA and lncRNA matrices of the encoded proteins were obtained using Perl software. The GSEA website was used to search for gene sets: extracted protein-encoded immune-related genes applying to IMMUNE_RESPONSE (M19817) and IMMUNE_SYSTEM_PROCESS (M13664). The R (version 3.6.1) and Bioconductor (https://www.bioconductor.org/) packets were used to obtain immune-related lncRNAs and for the corresponding data processing and analysis.

Analysis of the differential expression of lncRNAs

Differentially expressed lncRNAs in EAC were screened using the R-package "edgeR." The screening criteria were a log2 (foldchange) > 2 and a false discovery rate (FDR) < 0.05. Then, a volcanic map was plotted using the R-package "gplot2."

Single factor Multivariate Cox regression analysis, Lasso regression analysis and prognostic model construction

To screen differentially expressed immune-related lncRNAs, single factor Cox regression analysis was performed using the R-package "survival " with $P < 0.001$. To avoid overfitting, the statistically significant differentially expressed lncRNAs were also analyzed by lasso regression analysis. Finally, multivariate cox regression analysis was used to identify immune-related lncRNAs and construct a prognostic model. To evaluate the accuracy of the risk prognostic model, Kaplan-Meier (K-M) survival curves, operating characteristic (ROC)

curve, and independent prognostic analysis of clinical traits were performed. Towards that, all esophageal adenocarcinomas were divided into high-risk and low-risk groups according to their median risk score. At the same time, we calculated HR and 95% CI of key lncRNAs in the prognostic model, A *P*-value < 0.05 was considered statistically significant.

Evaluation of prognostic models, K-M survival analysis, and prognostic analysis of clinical traits

To assess the predictive ability of the prognostic model, K-M survival analysis was performed on the patient risk score. Next, the roc curve of the 5-year overall survival rate was plotted, and the area under the curve (AUC) as well as other clinical traits (gender, staging, TNM, and risk score) were calculated using the R package "survivalROC." An AUC value of 0.7 to 0.9 accuracy rate is generally considered medium accuracy, while an AUC value > 0.9 is considered high accuracy. In addition, to explore the value and significance of lncRNAs in predicting the prognosis of EAC, we performed K-M survival analysis of individual lncRNAs that were statistically significant as observed by the results of multivariate cox regression analysis. The clinical characters of EAC were analyzed by single factor and multiple factor cox regression analyses.

Results

Differentially expressed lncRNAs in EAC

A total of 56754 genes from 78 EAC tissues samples and 9 paracancerous or normal esophageal tissues were obtained from the TCGA database. Furthermore, clinical data were downloaded for 87 patients with EAC (Table 1). These data were processed and analyzed using the R language and the corresponding R packets to obtain 14131 immune-related lncRNAs and 19659 protein-encoded immune-related genes. Using the edgeR package, 1322 differentially expressed immune-related lncRNAs were screened with a threshold of |log2FC| > 1 and FDR < 0.05, including 28 up-regulated and 66 down-regulated lncRNAs (Fig. 1a). A total of 28 immune-related lncRNAs identified as prognostic risk factors were preliminarily screened using single factor Cox regression analysis combined with the corresponding clinical data (Table 2). In addition, 12 key immune-related lncRNAs were further identified by Lasso regression analysis (Fig. 1b and 1c).

Construction and evaluation of the prognostic model of EAC

All esophageal adenocarcinomas were divided into high- and low-risk groups according to the median risk score. Then, we constructed a prognostic model based on the patient's prognostic risk scores. A total of 12 lncRNAs were used for the risk scoring model with a risk score $=(1.84)*Exp_{LINC01612}+(-4.40)*Exp_{MIRLET7BHG}+(1.86)*Exp_{AL136115.1}+(1.86)*Exp_{AL121992.3}+(2.00)*Exp_{AC087620.1}+(1.16)*Exp_{AC005841.1}+(1.37)*Exp_{AC016394.1}+(1.21)*Exp_{AC079684.1}+(-1.15)*Exp_{AC078778.1}+(0.81)*Expression_{AC010168.1}+(1.26)*Expression_{AC048344.4}+(-0.89)*Exp_{AL163051.2}$. The K-M survival analysis ($P = 1.063e{-}10$, Fig. 5f) indicated that the overall survival time of the higher risk group was significantly shorter than that of the lower risk group. The area under the ROC curve of 5-year total survival rate was 0.90 (Fig. 2). Prognostic risk score predicted the independent prognostic risk for esophageal adenocarcinoma via single factor and multifactorial independent prognostic analysis,

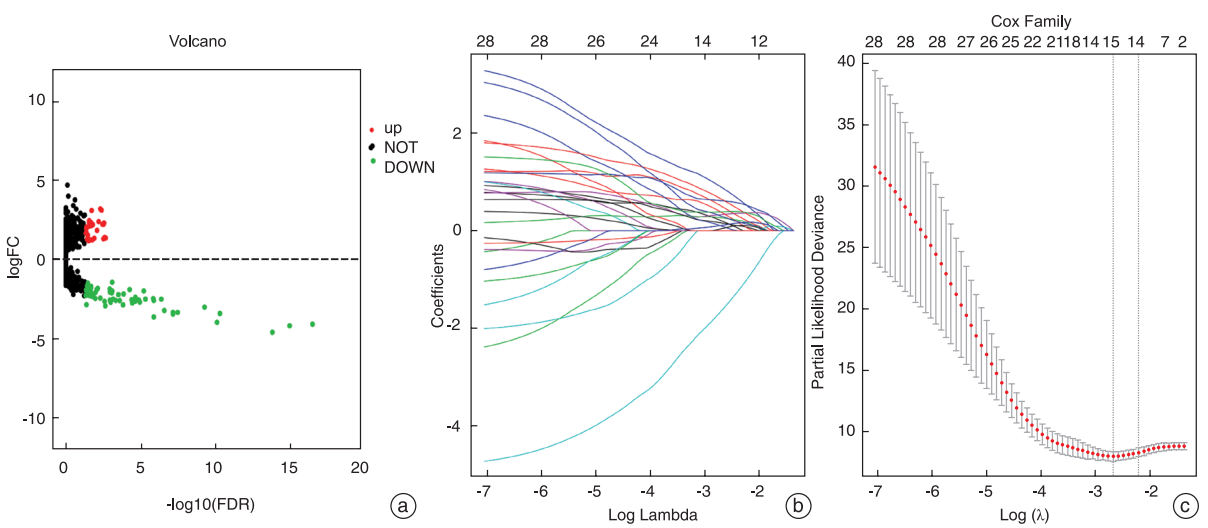

Fig. 1 Identification of the differentially expressed lncRNA by Lasso regression analysis in EAC. (a) Volcano plot of the differentially expressed lncRNAs; (b) tuning parameter (lambda) selection in the Lasso regression using 10 fold cross-validation via minimum criteria; (c) Lasso coefficient profiles of the features against the log2 (lambda)

Table 1 Clinical characteristics of esophageal adenocarcinoma

Clinical characteristics	*n* (%)
Gender	
Male	75 (86.2)
Female	12 (13.8)
Stage	
I	11 (12.6)
II	22 (25.3)
III	29 (33.3)
IV	5 (5.8)
Unknow	20 (23.0)
Tumor	
T1	24 (27.6)
T2	11 (12.6)
T3	37 (42.6)
T4	1 (1.1)
Unknow	14 (16.1)
Fustat	
Alive	43 (49.4)
Dead	44 (50.6)
Node	
N0	21 (24.1)
N1	40 (46.0)
N2	6 (6.9)
N3	5 (5.7)
Unknow	15 (17.3)
M	
M0	51 (58.6)
M1	5 (5.7)
Unknow	31 (35.7)

$P < 0.001$ (Fig. 3). The heatmap of 12 lncRNAs involved in constructing the risk scoring model is shown in Fig. 4. In addition, we also calculated the HR and 95% CI for these lncRNAs. Our results showed that among these 12 lncRNAs, 8 were independent prognostic risk factors for EAC ($P < 0.05$; Table 3).

Prognostic biomarkers of esophageal adenocarcinoma

Using a K-M survival analysis of 8 lncRNAs with independent prognostic risk factors, we further short-listed 5 immune-related lncRNAs with independent prognostic value: AL136115.1 ($P = 0.006$), AC079684.1 ($P = 0.008$), AC07916394.1 ($P = 0.0386$), AC087620.1 ($P = 0.041$) and MIRLET7BHG ($P = 0.044$). Based on our results, we identified a favorable prognostic biomarker, MIRLET7BHG, and four poor prognostic biomarkers (AL136115.1, AC079684.1, AC016394.1 and AC087620.1) (Fig. 5a–5e).

Table 2 Prognostic immune-related lncRNA in esophageal adenocarcinoma identified preliminary by univariate Cox regression analysis

Immune-related lncRNA name	HR	*P*
AC005841.1	2.640 (1.286–5.417)	0.008
AL136115.1	2.753 (1.361–5.570)	0.005
JPX	2.973 (1.393–6.346)	0.005
AL121992.3	3.275 (1.534–6.990)	0.002
MIRLET7BHG	0.285 (0.112–0.724)	0.008
AL080317.1	4.001 (2.019–7.926)	< 0.001
AC010168.1	2.534 (1.310–4.899)	0.006
AC048344.4	3.310 (1.337–8.197)	0.01
AL163051.2	3.234 (1.415–7.390)	0.005
AC079684.1	4.566 (1.932–10.787)	< 0.001
KCNQ1OT1	2.191 (1.290–3.720)	0.004
AC087752.4	2.728 (1.312–5.672)	0.007
AL133243.2	2.837 (1.438–5.598)	0.003
AL024508.2	1.785 (1.160–2.748)	0.008
AF117829.1	4.296 (1.645–11.221)	0.003
AC016394.1	2.597 (1.416–4.762)	0.002
AC078778.1	2.734 (1.290–5.793)	0.009
AC127024.3	2.311 (1.254–4.261)	0.007
AL590822.2	1.855 (1.215–2.831)	0.004
LINC01612	1.783 (1.166–2.726)	0.008
AC139100.2	2.741 (1.433–5.244)	0.002
AC087620.1	3.910 (1.642–9.309)	0.002
AL031673.1	2.056 (1.340–3.153)	< 0.001
ZNF337-AS1	3.150 (1.484–6.688)	0.003
AL596247.1	2.686 (1.394–5.174)	0.003
AC009318.2	3.699 (1.537–8.903)	0.004
AC012467.2	2.604 (1.522–4.455)	< 0.001
AC097468.3	3.344 (1.513–7.393)	0.003

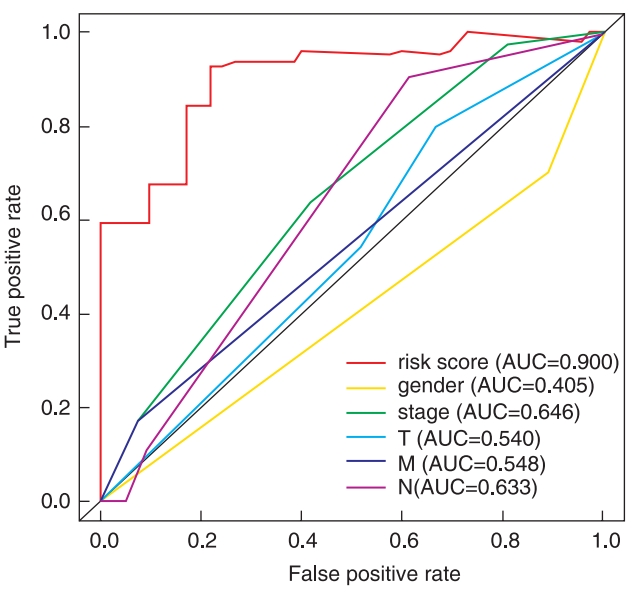

Fig. 2 ROC curve of multivariate Cox analysis model

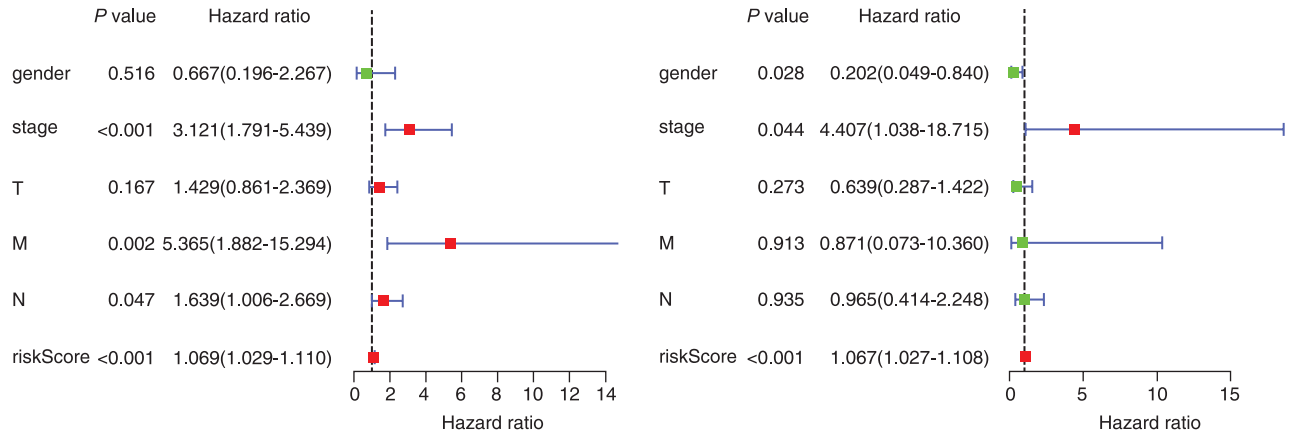

Fig. 3 Univariate and multivariate independent prognostic analysis of clinical features of esophageal adenocarcinoma

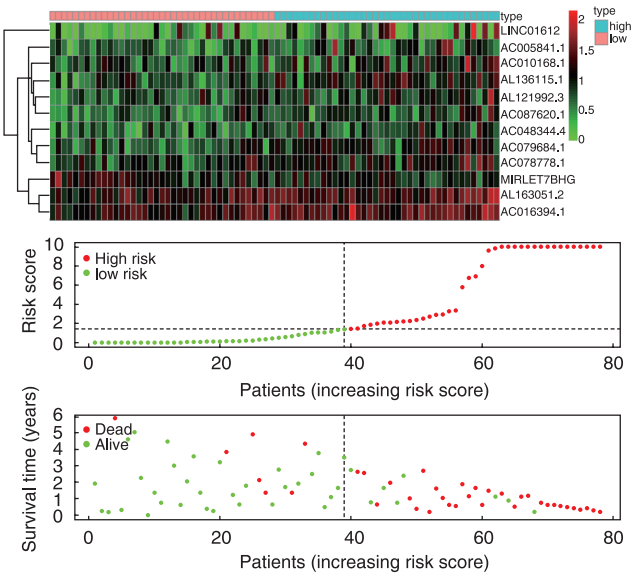

Fig. 4 Risk score and heat map of Immune-related lncRNA expression and scattered plots of survival time

Table 3 Result of the multivariate Cox regression analysis based on the 12 key immune-related lncRNA

immune-related lncRNA name	Coef	HR (95%CI)	*P*
LINC01612	1.842304116	6.311(3.150–12.643)	2.03E-07
MIRLET7BHG	-4.395979721	0.012(0.002–0.069)	5.95E-07
AL136115.1	1.862898963	6.442(2.414–17.193)	0.000199466
AL121992.3	1.857241154	6.406(2.088–19.652)	0.001165136
AC087620.1	2.001926502	7.403(1.902–28.814)	0.003885086
AC005841.1	1.157845653	3.183(1.356–7.471)	0.00782035
AC016394.1	1.369822912	3.934(1.338–11.575)	0.012837805
AC079684.1	1.210612392	3.355(1.033–10.896)	0.043959335
AC078778.1	-1.153082814	0.315(0.098–1.016)	0.053285834
AC010168.1	0.814394289	2.257(0.981–5.195)	0.055437015
AC048344.4	1.260896544	3.528(0.845–14.735)	0.083815226
AL163051.2	-0.891848958	0.410(0.128–1.310)	0.132527493

HR: hazard ratio; coef: coefficient

Discussion

Numerous studies have confirmed that lncRNAs play a wide range of regulatory roles in tumor occurrence, immune response, and tumor progression [12–14]. LncRNAs play a significant role in different stages of tumor immunity, such as antigen recognition, immune activation, immune cell infiltration, and tumor clearance [15]. Lv *et al* found that lncRNAs are involved in regulatory pathways of the immune system, such as T cell differentiation, immune deficiency, and cytotoxicity of natural killer cells, affecting patient's prognosis in hepatocellular carcinoma [16].

In this study, we obtained transcript data and clinical data from patients with esophageal adenocarcinoma from the TCGA database. Using correlation analysis, we found 14131 immune-related lncRNAs and 19659 protein-encoded immune-related genes in esophageal adenocarcinoma. We used univariate cox regression analysis and identified 28 immune-related lncRNAs that were associated with prognosis. In addition, K-M survival analysis (P = 1.063e–10) showed that the total survival time of the higher risk group was significantly shorter than that of the lower risk group. The area under the ROC curve of 5-year total survival rate was 0.90, indicating that the prediction accuracy of this prognostic model was relatively high. Prognostic risk score showed independent prognostic risk for esophageal adenocarcinoma via single factor and multifactorial independent prognostic analysis. In addition, the HR and 95% CI of each key immune-related lncRNA were calculated using multivariate Cox regression, and 12 key significant immune-related lncRNAs were identified. Moreover, K-M survival analysis identified five immune-related lncRNAs with independent prognostic value: a favorable prognostic biomarker, MIRLET7BHG, and four poor prognostic biomarkers (AL136115.1, AC079684.1,

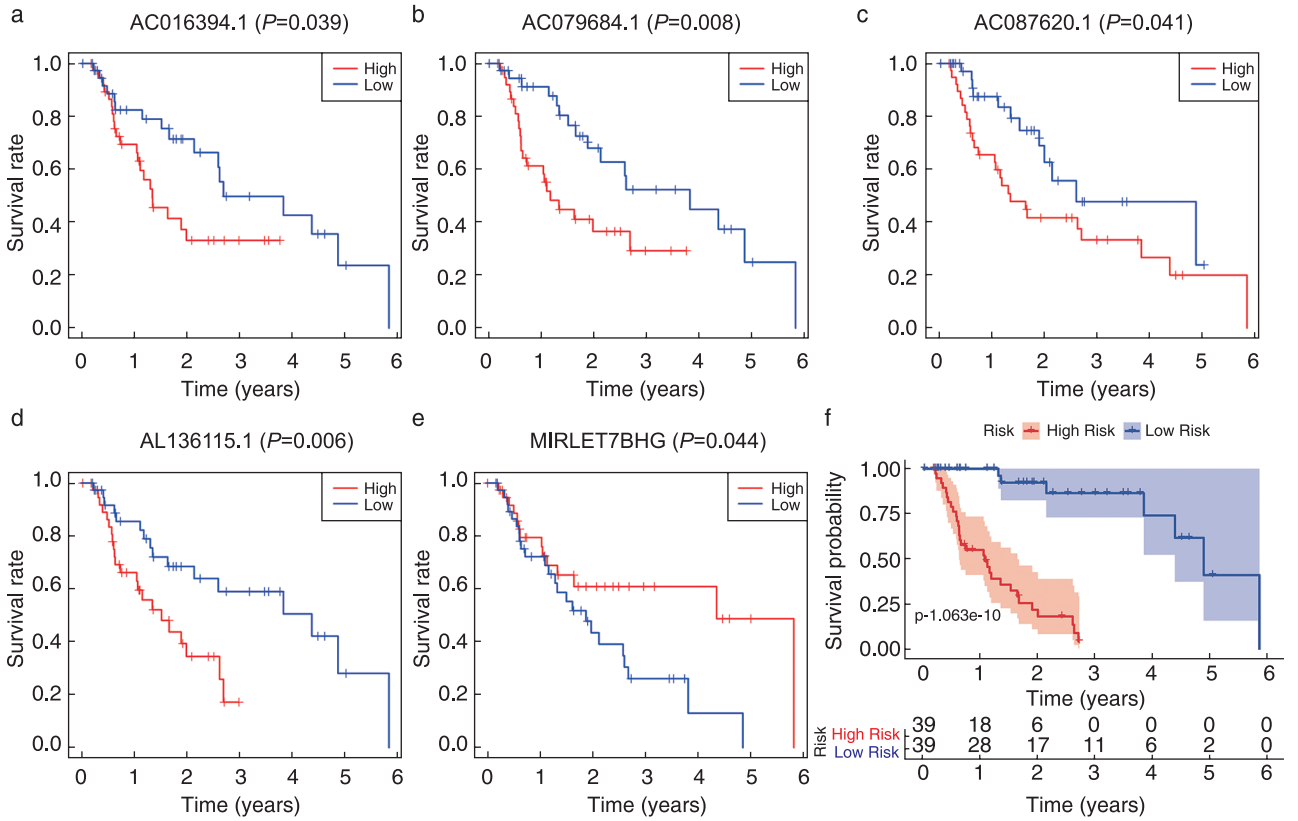

Fig. 5 K-M survival curves of the 8 significant key immune-related lncRNA identified using multivariate Cox regression and evaluation of the prognostic model of esophageal adenocarcinoma using the K-M survival curve

AC016394.1, and AC087620.1). Since there is a dearth of studies on these 4 immune-related lncRNAs [17–18], further research is needed to validate their role in the progression and prognosis of EAC disease. Liu et al. found that the MIRLET7BHG gene polymorphism may be an important predictor of asbestos exposure-related lung cancer [18]. Studies on lncRNA (MIRLET7BHG) have not been reported yet. Although immune-related lncRNAs are dysregulated during cell carcinogenesis, they are rarely reported in EAC [15, 19–20]. Wu *et al* reported that EAC exhibited reduced non-coding region methylation. Methylation of the long noncoding RNA AFAP1-AS1 is reduced in EAC, and its expression inhibits the cancer-related biological functions of EAC cells [19]. However, this study had some limitations. The conclusions were obtained from the TCGA database, and the prediction model and predictive markers of EAC lack domestic data for confirmation. Further, the role and mechanism of immune-related lncRNAs in EAC need to be further validated.

Conclusions

In summary, we screened lncRNAs from TCGA data base analyzed by various statistical tools. Based on our results, we identified 12 key immune-related lncRNAs in the present work and constructed a prognostic model of EAC with moderate predictive accuracy. In addition, we identified five immune-related lncRNAs as independent prognostic factors for EAC: AL136115.1, AC079684.1, AC016394.1, AC087620.1, and MIRLET7BHG. While MIRLET7BHG was identified as a favorable prognostic biomarker, the remaining four (AL136115.1, AC079684.1, AC016394.1, and AC087620.1) were identified as poor prognostic biomarkers.

Conflicts of interest

The authors indicated no potential conflicts of interest.

References

1. Bray F, Ferlay J, Soerjomataram I, *et al*. Global cancer statistics 2018: GLOBOCAN estimates of incidence and mortality worldwide for 36 cancers in 185 countries. CA Cancer J Clin, 2018, 68: 394–424.

2. Chen R, Zheng RS, Zhang SW, *et al*. Analysis of incidence and mortality of esophageal cancer in China, 2015. Chin J Prev Med (Chinese), 2019, 53: 1094–1097.
3. Gao X, Wang Z, Kong C, *et al*. Trends of esophageal cancer mortality in Rural China from 1989 to 2013: An age-period-cohort analysis. Int J Environ Res Public Health, 2017, 14: 218.
4. Zhang HY, Pei XF, Mo XQ, *et al*. Incidence and survival changes in patients with esophageal adenocarcinoma during 1984–2013. Biomed Res Int, 2019, 2019: 7431850.
5. Cowie A, Noble F, Underwood T. Strategies to improve outcomes in esophageal adenocarcinoma. Expert Rev Anticancer Ther, 2014, 14: 677–687.
6. Arnold M, Laversanne M, Brown LM, *et al*. Predicting the future burden of esophageal cancer by histological subtype: international trends in incidence up to 2030. Am J Gastroenterol, 2017, 112: 1247–1255.
7. Li H, Chen WQ. Progress in research of high risk assessment models for esophageal cancer. Chin Cancer (Chinese), 2019, 28: 883–890.
8. Yang FL, Hong K, Zhao GJ, *et al*. Construction of prognostic model and identification of prognostic biomarkers based on the expression of long non-coding RNA in bladder cancer via bioinformatics. J Peking Uni (Health Sci) (Chinese), 2019, 51: 615–622.
9. Li XM, Xing Y, ZA WJ, *et al*. Research progress of long non-coding RNA in esophageal cancer. Shandong Med J (Chinese), 2019, 59: 94–97.
10. Talebi A, Masoodi M, Mirzaei A, *et al*. Biological and clinical relevance of metastasis-associated long noncoding RNAs in esophageal squamous cell carcinoma: A systematic review. J Cell Physiol, 2020, 235: 848–868.
11. Yan YS, Li SB, Wang SH, *et al*. Long noncoding RNA HAND2-AS1 inhibits cancer cell proliferation, migration, and invasion in esophagus squamous cell carcinoma by regulating microRNA-21. J Cell Biochem, 2019, 120: 9564–9571.
12. Leucci E, Coe EA, Marine JC, *et al*. The emerging role of long non-coding RNAs in cutaneous melanoma. Pigment Cell Melanoma Res, 2016, 29: 619–626.
13. Li X, Meng Y. Survival analysis of immune-related lncRNA in low-grade glioma. BMC Cancer, 2019, 19: 813.
14. Wang B, Liang T, Li J. Long noncoding RNA LINC01296 is associated with poor prognosis in ESCC and promotes ESCC cell proliferation, migration and invasion. Eur Rev Med Pharmacol Sci, 2018, 22: 4524–4531.
15. Yu WD, Wang H, He QF, *et al*. Long noncoding RNAs in cancer-immunity cycle. J Cell Physiol, 2018, 233: 6518–6523.
16. Lv Y, Wei W, Huang Z, *et al*. Long non-coding RNA expression profile can predict early recurrence in hepatocellular carcinoma after curative resection. Hepatol Res, 2018, 48: 1140–1148.
17. Feng Q, Zhang H, Yao D, *et al*. Emerging role of non-coding RNAs in esophageal squamous cell carcinoma. Int J Mol Sci, 2019, 21: 258.
18. Liu CY, Stucker I, Chen C, *et al*. Genome-wide gene-asbestos exposure interaction association study identifies a common susceptibility variant on 22q13.31 associated with lung cancer risk. Cancer Epidemiol Biomark Prev, 2015, 24: 1564–1573.
19. Wu W, Bhagat TD, Yang X, *et al*. Hypomethylation of noncoding DNA regions and overexpression of the long noncoding RNA, AFAP1-AS1, in Barrett's esophagus and esophageal adenocarcinoma. Gastroenterology, 2013, 144: 956–966.
20. Li S, Xu Y, Sun Z, *et al*. Identification of a lncRNA involved functional module for esophageal cancer subtypes. Mol Biosyst, 2016, 12: 3312–3323.

DOI 10.1007/s10330-020-0408-8
Cite this article as: Qin K, Cheng Y, Zhang J, *et al*. Prognostic risk model construction and prognostic biomarkers identification in esophageal adenocarcinoma based on immune-related long noncoding RNA. Oncol Transl Med, 2020, 6: 109–115.

Oncology and Translational Medicine
DOI 10.1007/s10330-019-0381-1

June 2020, Vol. 6, No. 3, P116–P120

ORIGINAL ARTICLE

Peritoneal cancer index is a prognostic indicator of survival in advanced gastric cancer with peritoneal carcinomatosis

Guangcai Niu, Xiangdong Ma (✉)

Department of Oncological Surgery, Xuzhou Central Hospital, Xuzhou 221009, China

Abstract

Objective The peritoneal cancer index (PCI) has been used for the detailed evaluation of the peritoneal spread in tumors of a gynecologic origin and has been found to be a prognostic indicator of survival. The aim of this study was to identify the significance of the PCI in advanced gastric cancer (AGC) with peritoneal carcinomatosis (PC).

Methods From 2010 to 2018, a retrospective analysis was carried out of 60 AGC patients with PC, including 21 patients with a PCI ≤ 13 and 39 with a PCI > 13. All patients were treated with both surgery and intraoperative peritoneal hyperthermic chemotherapy (IPHC). The performance status (Karnofsky performance status), age, sex, Borromann's classification, differentiation, depth of invasion, lymph node metastasis, PCI, extent of gastrectomy, extent of lymph node dissection, and residual tumor volume were retrospectively evaluated and correlated to survival.

Results The overall 5-year survival rate was 43% and mean survival was (54.47 ± 4.53) months. The favorable clinical prognostic indicators of survival were Borromann's classification, differentiation, depth of invasion, PCI, and residual tumor volume on univariate analyses (P < 0.05). The Cox proportional regression hazard model showed that only the volume of residual tumor and PCI were associated with postoperative survival. The median survival time was 69.76 months for patients with a PCI ≤ 13 and 39.96 months for patients with a PCI > 13. There was a significant difference in survival rate between the two group (P = 0.004). Postoperative major morbidity and mortality rates were 23.81% and 4.76% in the PCI ≤ 13 group and 43.59% and 5.12% in the PCI > 13 group, respectively.

Conclusion The peritoneal spread in advanced gastric cancer with peritoneal carcinomatosis can be assessed in detail using the PCI. It is also a significant prognostic factor of survival and is useful in identifying subgroups.

Received: 4 September 2019
Revised: 2 March 2020
Accepted: 16 March 2020

Key words: peritoneal cancer index (PCI); advanced gastric cancer (AGC); peritoneal carcinomatosis (PC); survival; complication

The incidence of gastric cancer is increasing year by year, ranking first in the incidence of gastrointestinal malignant tumors, and the mortality rate is the second highest of all cancers [1]. Peritoneal carcinomatosis (PC) is one of the most predominant means of metastasis in gastric cancer, diagnosed in 5%–20% of patients and is considered a fatal disease with limited treatment options [2–3]. It also has the most frequent pattern of postoperative recurrence, which is the major cause of death in advanced gastric cancer (AGC) with PC [4].

A meta-analysis demonstrated that intraoperative peritoneal hyperthermic chemotherapy (IPHC) combined with surgery had a positive effect on overall survival [5]. However, high morbidity and mortality after this treatment was also reported [6]. Surgeons must, therefore, select patients carefully to achieve a balance between the postoperative risks of the combined treatment and the potential benefits in survival and quality of life.

The peritoneal cancer index (PCI) is used to determine if surgical intervention should be attempted as a cure or if a palliation move is more suitable for cancer patients [6–7]. The aim of the present study is to identify the significance of the PCI for the detailed evaluation of peritoneal spread and for selecting AGC patients with PC who would

✉ Correspondence to: Xiangdong Ma. Email: m10046@sina.com

benefit from surgery.

Patients and methods

From 2010 to 2018, 60 patients [mean age (49 ± 9.42) years, range 30–70 years], were treated for AGC with PC. The performance status (Karnofsky performance status), age, sex, Borromann's classification, differentiation, depth of invasion (T), lymph node metastasis (N), PCI, extent of gastrectomy, extent of lymph node dissection, and residual tumor volume were retrospectively evaluated and correlated to survival. The diagnosis and staging of AGC with PC was made by physical examination, hematological-biochemical examinations, tumor markers, and computed tomography (CT) scan. All patients received adjuvant chemotherapy based on platinum and fluorouracil after surgery. Patients who received palliative bypass operations, those aged over 70 years, those with extra-abdominal metastases and liver metastases, those who failed to follow-up, and those whom in severe condition (renal or myocardial failures etc.) were excluded from the study.

All patients received IPHC, which was performed immediately after surgical resection and intestinal reconstruction. Briefly, two inflow tubes were placed in the subphrenic cavity and one outflow tube was placed within the Douglas' pouch. Approximately 5–6 L of perfusate containing cisplatin (50 g/mL) and mitomycin (5 g/mL) with an invariable velocity (500–600 mL/min) was circulated for 60 min. The peritoneal temperature was maintained at 43 °C. After the intraoperative perfusion, the abdomen was suctioned dry of fluid.

The TNM staging system, according to the Union for International Cancer Control (UICC), was used to describe the operative findings and pathological diagnosis [8]. The determination of the absence or presence of peritoneal metastasis and the extent of lymph node dissection was based on the Japanese Classification of Gastric Carcinoma [9].

The PCI was calculated intraoperatively. This index is calculated according to the size of the lesions and the quadrants in which they are found. A score is allocated according to whether a lesion is seen in the central abdominal area, right upper quadrant, epigastrium, left upper quadrant, left flank, left lower quadrant, pelvis, right lower quadrant, right flank, upper jejunum, lower jejunum, upper ileum, or lower ileum. The score is dependent on the size of the preoperative tumor nodule. A score of 1 is given to lesion sizes up to 0.5 cm, a score of 2 is allocated to tumor sizes 0.5–5.0 cm, and a score of 3 is given to lesions > 5.0 cm or confluence. The sum of the scores equals the PCI. Residual disease that was unresectable was scored according to the completeness of cytoreduction (CC) score. This score is calculated using the size of the residual tumor nodules seen macroscopically after cytoreduction; CC-0 is no nodules seen, CC-1 is nodules < 2.5 mm, CC-2 is nodules between 2.5 mm and 25 mm; and CC-3 is nodules > 25 mm. Tissue samples taken intraoperatively were sent for histopathological analysis [10]. Patients were divided into two groups according to PCI.

Statistical analysis was carried out using SPSS 13.0 software (SPSS Inc, Chicago, USA). The χ^2 test was used for the comparison of the two groups. Postoperative survival curves were generated according to the Kaplan-Meier method and compared using the log-rank test. Independent prognostic factors were analyzed by the Cox proportional regression hazard method. $P < 0.05$ was considered to indicate statistical significance.

Results

The median overall survival was 54.47 months for the entire cohort, with 1-, 3-, and 5-year survival rates of 85%, 61%, and 43%, respectively. In order to assess the impact of different PCI for AGC patients with PC, we then performed a matched-paired analysis. Specifically, AGC patients with a PCI ≤ 13 were matched for performance status (Karnofsky performance status), age, sex, Borromann's classification, differentiation, depth of invasion, lymph node metastasis, PCI, extent of gastrectomy, extent of lymph node dissection, and residual tumor volume with patients with a PCI > 13 (Table 1). All patients underwent gastrectomy for the resection of the primary tumor, 38 of a subtotal manner and 22 of total. Small residual cancer volume was performed in 13 cases of the 21 patients in the PCI ≤ 13 group, 18 cases of the 39 patients in the PCI > 13 group.

The median survival time was 69.76 months in patients with a PCI ≤ 13 and 39.96 months in patients with a PCI > 13. There was a significant difference in survival rates between the two groups ($P = 0.004$; Fig. 1). The Borromann's classification, differentiation, depth of invasion, PCI, and volume of residual tumor were found to correlate with survival in the univariate analyses (Table 2). Age, sex, performance status, lymph node metastasis, extent of gastrectomy, and extent of lymph node dissection were not related to survival ($P > 0.05$). Moreover, while not significant, patients with an early lymph node metastasis stage tended to have increased survival compared to late stage ($P = 0.103$). The Cox proportional regression hazard model showed that a small volume of residual tumor and lower PCI were independent prognostic factors of survival (Table 2).

Table 3 shows the morbidity and mortality rates. Patients in both groups developed many complications after surgery; however, the morbidity and mortality rates with a PCI ≤ 13 were lower than those with PCI > 13, with

Table 1 Comparison of AGC patients with PC between PCI ≤ 13 and PCI > 13

	PCI ≤ 13	PCI > 13	*P*
Gender			0.316
Male	9	22	
Female	12	17	
Performance status			0.515
Score 90–100	11	17	
Score 70–80	10	22	
Borromann's classification			0.392
I + II	7	9	
III + IV	14	30	
Differentiation			0.635
Well	5	6	
Moderately	10	18	
Poorly	6	15	
Depth of invasion (T)			0.679
T3	7	11	
T4	14	28	
Lymph node metastasis (N)			0.628
N1	5	6	
N2	12	27	
N3	4	6	
Gastrectomy			0.064
Subtotal	10	28	
Total	11	11	
Extent of lymph node dissection			0.643
D1	6	3	
D2	13	26	
D3	2	10	
Residual tumor			0.244
CC-0 + CC-1	13	18	
CC-2 + CC-3	8	21	

a significant difference in the incidence of complications ($P = 0.016$). Postoperative major morbidity and mortality rates were 23.81% and 4.76% in the PCI ≤ 13 group and 43.59% and 5.12% in the PCI > 13 group, respectively. One death was directly related to respiratory failure,

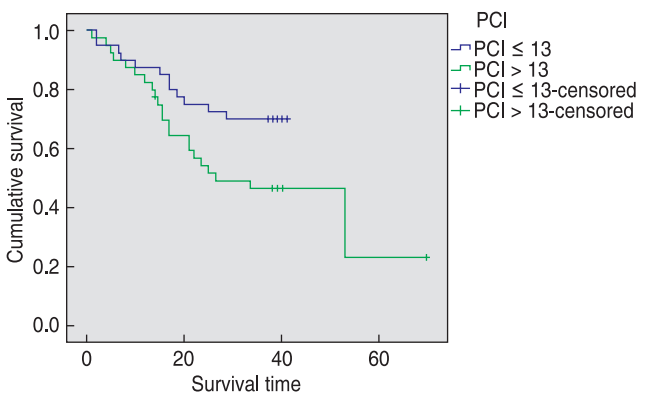

Fig. 1 The comparison of survival time between PCI ≤ 13 and PCI > 13

Table 2 Univariate analysis and Cox multivariate analysis to identify independent prognostic factors

	Median survival	Univariate *P*	Multivariate *P*
Gender		0.279	
Male	48.64		
Female	59.51		
Performance status		0.315	
Score 90–100	59.35		
Score 70–80	48.97		
Borromann's classification		0.048	0.596
I + II	63.83		
III + IV	42.95		
Differentiation		0.002	0.090
Well	72.50		
Moderately	47.29		
Poorly	24.38		
Depth of invasion (T)		0.006	0.118
T3	69.70		
T4	42.14		
Lymph node metastasis (N)		0.103	
N1	70.00		
N2	44.07		
N3	27.88		
Gastrectomy		0.309	
Subtotal	51.23		
Total	56.10		
Extent of lymph node dissection		0.099	
D1	74.50		
D2	48.54		
D3	33.13		
PCI		0.004	0.030
PCI ≤ 13	69.76		
PCI > 13	39.96		
Residual tumor		0.000	0.037
CC-0 + CC-1	74.49		
CC-2 + CC-3	37.41		

Table 3 The morbidity and mortality of AGC patients with PC between PCI ≤ 13 and PCI > 13

	PCI ≤ 13	PCI > 13	*P*
Morbidity	5 (23.81%)	17 (43.59%)	0.016
Wound abscess	0	1	
Ileus	1	4	
Anastomotic failure	1	4	
Bleeding	1	3	
Pancytopenia	0	1	
Cardiac & respiratory dysfunction	1	2	
Others	1	2	
Mortality	1 (4.76%)	2 (5.12%)	N.S.
Cardiac & respiratory failure	1	0	
Bleeding	0	1	
Others	0	1	

Note: N.S., no significance

resulting in multi-organ failure in the PCI ≤ 13 group. There were 2 deaths in the PCI > 13 group, 1 died of liver failure and the other abdominal bleeding.

All the patients which survived surgery were assessed every 3 months with physical examinations, hematological-biochemical examinations, tumor markers, and CT-scanning. Patient's follow-up period (from surgery to the date of death or the end of the study) was between 5 and 79 months (median: 29 months).

Discussion

The prevalence of PC has been estimated at 22% in gastric cancer patients and even after extensive resections, approximately 50% of patients die from recurrent disease within the first 2 years after surgery [11–13]. Several studies have demonstrated the efficacy of IPHC with improvements both in the survival rate and a decrease in the incidence of peritoneal recurrence of AGC patients with PC [14–16]. However, combining two aggressive procedures can lead to greater mortality and morbidity rates, with morbidity rates as high as 60% [17]. Therefore, surgeons must carefully select patients to achieve a balance between the postoperative risks of extensive surgery and the potential benefits in survival and quality of life.

The PCI gives valuable information about the exact distribution of seeding and tumor volume, representing in detail the extent of peritoneal spread. It has been used for the evaluation of spread at the peritoneal surfaces in peritoneal mesothelioma, colorectal cancer, and other cancers. In some studies, they have demonstrated a PCI around 10 is of prognostic significance for many malignant tumors with peritoneal spread [18–19]. Therefore, this value is used to determine if surgical intervention should continue as an attempt at curing the peritoneal metastases or whether the intervention should be for palliation only. The PCI is also a crucial prognostic indicator in the AGC with PC. In our study, we found that there was a significant difference in the survival rates between the PCI ≤ 13 and PCI > 13 groups. The median survival time was 69.76 months in patients with a PCI ≤ 13 and 39.96 months in patients with PCI > 13.

Survival was significantly influenced by the residual volume of tumors and PCI. Completeness of excision was found to be significant, improving 3-year survival from 13% to 52% [20]. For AGC patients without residual macroscopic metastases, the cytoreductive surgery plus IPHC procedure can improve postoperative survival rate and decrease the incidence of peritoneal recurrence, and is an independent prognostic factor for these patients. When the resection does result in sufficient reduction in tumor volume, IPHC does not seem to be beneficial as the gain in terms of survival is minimal [21]. Generally speaking, cytoreductive surgery is performed to treat the macroscopic disease and IPHC to treat the microscopic residual disease to eradicate the disease completely during a single procedure. It is verified in our article that a large volume residual tumor remaining results in reduced survival. This study, and also previously reported data, showed that only cytoreductive surgery achieves an R0 or R1 resection, with the intent to cure, the combination of IHPC can improve survival rate [22–24].

However, high morbidity and mortality rates after cytoreductive surgery combined with IPHC have been reported [23, 25]. Some reports suggest that postoperative complications, including anastomotic leakage, bowel perforation, renal dysfunction, respiratory failure, and other complications occur more frequently when IPHC is applied [26–28], while others claim the combination is safe [29–30]. In our study, the morbidity and mortality rates were significantly higher in the group with a PCI > 13 than those with a PCI ≤ 13 (P = 0.016). This was likely due to the extent of surgery being larger in the PCI > 13 group, causing more damage. Jacquet *et al* [31] reported the morbidity and mortality in patients with adenocarcinoma of the colon and appendix was 35% and 5% when IPHC was applied.

Several limitations in this study should be addressed. Firstly, all the patients included in this study were without extra-abdominal metastases and liver metastases. As such, results from this paper may not be extensively representative across the entire AGCs. Moreover, this study is a retrospective study with a small number of cases. Large sample multi-center randomized controlled studies are required to further verify the efficacy and safety of surgery and IPHC in AGCs.

The PCI is a significant predictor of survival in AGC patients with PC. Using PCI as a detailed evaluation of the peritoneal spread is possible. On the whole, surgery plus IPHC for AGC with PCI ≤ 13 is a relatively safe procedure.

Acknowledgment

The study was supported by the Department of Oncological Surgery, Xuzhou Central Hospital, Xuzhou, China.

Conflicts of interest

The authors indicated no potential conflicts of interest.

References

1. Meng LJ, Shen FZ. Expression and clinical significance of serum lipoprotein (a) in patients with gastric cancer. Oncol Transl Med, 2018, 4: 242–246.
2. Yonemura Y, Canbay E, Li Y, *et al*. A comprehensive treatment for peritoneal metastases from gastric cancer with curative intent. Eur J Surg Oncol, 2016, 42: 1123–1131.

3. Goéré D, Gras-Chaput N, Aupérin A, *et al*. Treatment of gastric peritoneal carcinomatosis by combining complete surgical resection of lesions and intraperitoneal immunotherapy using catumaxomab. BMC Cancer, 2014, 14: 148.
4. Yoo CH, Noh SH, Shin DW, *et al*. Recurrence following curative resection for gastric carcinoma. Br J Surg, 2000, 87: 236–242.
5. Yan TD, Black D, Sugarbaker PH, *et al*. A systematic review and meta-analysis of the randomized controlled trials on adjuvant intraperitoneal chemotherapy for resectable gastric cancer. Ann Surg Oncol, 2007, 14: 2702–2713.
6. Glehen O, Gilly FN, Arvieux C, *et al*. Peritoneal carcinomatosis from gastric cancer: a multi-institutional study of 159 patients treated by cytoreductive surgery combined with perioperative intraperitoneal chemotherapy. Ann Surg Oncol, 2010, 17: 2370–2377.
7. Leiting JL, Grotz TE. Optimizing outcomes for patients with gastric cancer peritoneal carcinomatosis. World J Gastrointest Oncol, 2018, 10: 282–289.
8. Sobin LH, Wittekind Ch ed. UICC TNM classification of malignant tumors, 5 ed. New York: Wiley, 1997. 59–62.
9. Japanese Gastric Cancer Association. Japanese classification of gastric carcinoma (2nd English edition). Gastric Cancer, 1998, 1: 10–24.
10. Begossi G, Gonzalez-Moreno S, Ortega-Perez G, *et al*. Cytoreduction and intraperitoneal chemotherapy for the management of peritoneal carcinomatosis, sarcomatosis and mesothelioma. Eur J Surg Oncol, 2002, 28: 80–87.
11. Kuramoto M, Shimada S, Ikeshima S, *et al*. Extensive intraoperative peritoneal lavage as a standard prophylactic strategy for peritoneal recurrence in patients with gastric carcinoma. Ann Surg, 2009, 250: 242–246.
12. Rajdev L. Treatment options for surgically resectable gastric cancer. Curr Treat Options Oncol, 2010, 11: 14–23.
13. Shiozaki H, Elimova E, Slack RS, *et al*. Prognosis of gastric adenocarcinoma patients with various burdens of peritoneal metastases. J Surg Oncol, 2016, 113: 29–35.
14. Desiderio J, Chao J, Melstrom L, *et al*. The 30-year experience – A meta-analysis of randomised and high-quality non-randomised studies of hyperthermic intraperitoneal chemotherapy in the treatment of gastric cancer. Eur J Cancer, 2017, 79: 1–14.
15. Bonnot PE, Piessen G, Kepenekian V, *et al*. Cytoreductive surgery with or without hyperthermic intraperitoneal chemotherapy for gastric cancer with peritoneal metastasis (CYTO-CHIP study): A propensity score analysis. J Clin Oncol, 2019, 37: 2028–2040.
16. Ychou M, Boige V, Pignon JP, *et al*. Perioperative chemotherapy compared with surgery alone for resectable gastroesophageal adenocarcinoma: An FNCLCC and FFCD multicenter phase III trial. J Clin Oncol, 2011, 29: 1715–1721.
17. Sebbag G, Sugarbaker PH. Peritoneal mesothelioma proposal for a staging system. Eur J Surg Oncol, 2001, 27: 223–224.
18. Coccolini F, Cotte E, Glehen O, *et al*. Intraperitoneal chemotherapy in advanced gastric cancer. Meta-analysis of randomized trials. Eur J Surg Oncol, 2014, 40: 12–26.
19. Grotz TE, Fournier KF, Mansfield PF. Patient selection for cytoreductive surgery. Surg Oncol Clin N Am, 2018, 27: 443–462.
20. Beaujard AC, Glehen O, Caillot JL, *et al*. Intraperitoneal chemohyperthermia with mitomycin C for digestive tract cancer patients with peritoneal carcinomatosis. Cancer, 2000, 88: 2512–2519.
21. Elias D, Blot F, Otmany AE, *et al*. Curative treatment of peritoneal carcinomatosis arising from colorectal cancer by complete resection and intraperitoneal chemotherapy. Cancer, 2001, 92: 71–76.
22. Cavaliere F, Perri P, Filippo FD, *et al*. Treatment of peritoneal carcinomatosis with intent to cure. J Surg Oncol, 2000, 74: 41–44.
23. Witkamp AJ, de Bree E, Kaag MM, *et al*. Extensive cytoreductive surgery followed by intra-operative hyperthermic intraperitoneal chemotherapy with mitomycin-C in patients with peritoneal carcinomatosis of colorectal origin. Eur J Cancer, 2001, 37: 979–984.
24. Yang XJ, Huang CQ, Suo T, *et al*. Cytoreductive surgery and hyperthermic intraperitoneal chemotherapy improves survival of patients with peritoneal carcinomatosis from gastric cancer: final results of a phase III randomized clinical trial. Ann Surg Oncol, 2011, 18: 1575–1581.
25. Schmidt U, Dahlke MH, Klempnauer J, *et al*. Perioperative morbidity and quality of life in long-term survivors following cytoreductive surgery and hyperthermic intraperitoneal chemotherapy. Eur J Surg Oncol, 2005, 31: 53–58.
26. Kunisaki C, Shimada H, Nomura M, *et al*. Lack of efficacy of prophylactic continuous hyperthermic peritoneal perfusion on subsequent peritoneal recurrence and survival in patients with advanced gastric cancer. Surgery, 2002, 131: 521–528.
27. Sugarbaker PH, Alderman R, Edwards G, *et al*. Prospective morbidity and mortality assessment of cytoreductive surgery plus perioperative intraperitoneal chemotherapy to treat peritoneal dissemination of appendiceal mucinous malignancy. Ann Surg Oncol, 2006, 13: 635–644.
28. Gori J, Castaño R, Toziano M, *et al*. Intraperitoneal hyperthermic chemotherapy in ovarian cancer. Int J Gynecol Cancer, 2005, 15: 233–239.
29. Kecmanovic DM, Pavlov MJ, Ceranic MS, *et al*. Treatment of peritoneal carcinomatosis from colorectal cancer by cytoreductive surgery and hyperthermic perioperative intraperitoneal chemotherapy. Eur J Surg Oncol, 2005, 31: 147–152.
30. Zhu ZG, Tang R, Yan M, *et al*. Efficacy and safety of intraoperative peritoneal hyperthermic chemotherapy for advanced gastric cancer patients with serosal invasion. A long-term follow-up study. Dig Surg, 2006, 23: 93–102.
31. Jacquet P, Stephens AD, Averbach AM, *et al*. Analysis of morbidly and mortality in 60 patients with peritoneal carcinomatosis treated by cytoreductive surgery and heated intraoperative intraperitoneal chemotherapy. Cancer, 1996, 77: 2622–2629.

DOI 10.1007/s10330-019-0381-1
Cite this article as: Niu GC, Ma XD. Peritoneal cancer index is a prognostic indicator of survival in advanced gastric cancer with peritoneal carcinomatosis. Oncol Transl Med, 2020, 6: 116–120.

Oncology and Translational Medicine
DOI 10.1007/s10330-020-0419-9

June 2020, Vol. 6, No. 3, P121–P125

ORIGINAL ARTICLE

Effects of MIF on proliferation, migration, and STAT1 pathway of colon cancer cells

Feng Liu (✉), Jianxin Zhong, Jianbin Sun, Hailong Wu

Department of Thyroid and Breast Surgery, Wuhan Puai Hospital, Tongji Medical College, Huazhong University of Science and Technology, Wuhan 430000, China

Abstract

Objective This study aimed to investigate how macrophage migration inhibitory factor (MIF) regulates the interaction of signal transducer and activator of transcription 1 (STAT1) with CD74, and affects colon cancer proliferation and invasion.

Methods After transfecting MIF small interfering RNA into the SW480 cell line, the expression of STAT1 and CD74 mRNA was detected by qRT-PCR and western blotting. Transwell and MTT assays were performed to detect the colon cancer cell invasion and proliferation ability. Co-immunoprecipitation was used to detect the interaction between CD74 and STAT1 proteins in the treated and control groups.

Results The cellular biological assays (MTT and Transwell) showed that the proliferation and invasion ability of colon cancer cells decreased after MIF knockdown; the results showed significant statistical difference ($P < 0.05$). The results of the co-immunoprecipitation assay suggested that MIF knockdown in colon cancer cells could inhibit the binding of CD74 and STAT1 proteins; statistical difference was observed between the two groups ($P < 0.05$).

Conclusion MIF can increase the proliferation and invasion of colon cancer cells by promoting the combination of CD74 and STAT1.

Received: 16 April 2020
Revised: 4 May 2020
Accepted: 23 May 2020

Key words: colon cancer; migration inhibitory factor; signal transducer and activator of transcription 1; cell proliferation; cell migration

Colon cancer is one of the most common malignant tumors; its morbidity ranks fourth among all the tumors in China [1]. As colon cancer typically exhibits locally infiltrating or distant metastasis, patients often need surgery. Prevention of rapid growth, metastasis, and recurrence of colon cancer are crucial to improve the prognosis of patients [2–3]. Therefore, curbing the proliferation and invasion ability of colon cancer cells has been a research focus in recent years. Macrophage migration inhibitory factor (MIF) can be rapidly secreted under the stimulation of extracellular microbial products or hypoxia environments, and binds to specific receptors to initiate downstream signal pathways that affect oncogenesis and tumor progression through interaction with tumor-related proteins [4–5]. Studies have shown that CD74 can act as a membrane receptor for MIF, which promotes the interaction of CD74 with transcription factors that regulate related downstream gene expression in cells [6–8]. Signal transducer and activator of transcription 1 (STAT1) was one of the first members of the STAT family to be discovered and studied. It is an important intracellular transcription factor that regulates tumor cell proliferation, apoptosis, and differentiation [9–10]. Our previous research has demonstrated the physical interaction of STAT1 and CD74 proteins in colon cancer cells. However, the role played by MIF in CD74/STAT1-mediated colon cancer invasion and metastasis needed further confirmation.

Materials and methods

Main experimental cells, materials, and reagents

Cell line

The human colon cancer cell line SW480 was purchased from ATCC.

Reagents

DMEM medium and fetal bovine serum were

✉ Correspondence to: Liu Feng. Email: lf5806@sina.com

purchased from GIBCO, USA. Small interfering RNAs (siRNAs) of MIF, STAT1, and CD74 were purchased from Wuhan Qingke Biotechnology Company. pCMV-Myc and pCMV-HA vectors were purchased from Shanghai Shuomeng Biological Company. pTalluc-DDR2 vector was purchased from Shanghai Bi Yuntian Biological Company. Polyclonal antibodies against HA-tag and anti-Myc were purchased from GIBCO, USA. Horseradish peroxidase (HRP) -conjugated goat anti-mouse IgG, HRP-conjugated goat anti-rabbit IgG, Anti-HA, and anti-Myc monoclonal antibodies were purchased from Wuhan Baoshide Company. A Lipofectamine 2000 transfection kit was purchased from Santa Cruz. Real-time quantitative PCR and reverse transcription were suitable for purchase from Japan's TAKARA Company. Immunochemoluminescence development reagent kits were purchased from Clontech, USA.

Instruments

A gel imaging system was purchased from Sigma, USA. Protein-A/G was purchased from Santa Cruz, USA. An LSLS-B50L vertical circular pressure steam sterilizer was purchased from Tuttnauer Company, USA. An all-around high-performance benchtop refrigerated centrifuge (Heaeus, Biofuge Stratos, Germany), a UV spectrophotometer (2540MK, Tuttnauer, USA), and a fluorescence analyzer (SCW-HS-840 type, OLYMPUS, Japan) were used in the experiments.

Research methods

Cell culture

Colon cancer cells were cultured with DMEM medium containing 10% fetal bovine serum and antibiotics (100 μg/mL streptomycin and 100 U/mL penicillin), in a 37 °C 5% CO_2 incubator. The cells were passaged when the cell density reached 70% or more. After washing with the medium, the cells were digested with trypsin containing 0.02% EDTA for 2 to 3 min. The digested cells were mixed with the same volume of serum-containing medium to terminate the digestion. The cells were then observed under a microscope. The adherent cells were pipetted, and centrifuged at 10,000 r/min for 5 min to remove the supernatant. Thereafter, the cell suspension was counted and inoculated into a new culture flask to continue the cultivation.

Transfection

When the colon cancer cells reached 70% density, they were transfected with siRNAs or overexpression plasmids of STAT1 and CD74. A 10 μg DNA sample was diluted and mixed with 240 μL serum-free DMEM medium, and incubated for 5 min. Then, 10 μL Lipofectamine 2000 transfection reagent was diluted with 250 μL DMEM without antibiotics and serum. After incubation for 5 min, the two solutions were mixed and incubated at room temperature for 20 min. The medium in a six-well plate was replaced with DMEM containing the transfection mixture, and the plate was placed into an incubator. After 6 h of culturing, the medium was discarded and the culturing was continued using DMEM containing 10% fetal bovine serum. Solutions A and B were configured according to the ratios 2 μL Lipo2000 + 100 μL Opti-MEM and 2.5 μL siRNA/NC + 100 μL Opti-MEM, respectively, and incubated at 37 °C for 5 min. Solutions A and B were gently mixed and incubated at 37 °C for 15 min. Then, 200 μL of the mixed liquid was added to each well, shaken, and incubated at 37 °C for 4–6 h.

Quantitative real-time PCR

Total RNA was isolated from cells using Trizol (Invitrogen). Reverse transcriptions were performed using a PrimeScript™ RT reagent kit (Takara, Dalian, China) according to the manufacturer's instructions. RT-PCR assays were performed under the following conditions: 37 °C for 15 min, 85 °C for 5 s, and 4 °C for 10 min. qRT-PCR was performed with SYBR®Premix Ex Taq™ (TaKaRa), according to the manufacturer's protocol, on an Applied Biosystems StepOne-Plus Real-Time PCR System. GAPDH was used as the loading control. Each reaction was done in triplicate.

Invasion assay

A 500 μL sample of serum-free DMEM medium was added to a 24-well plate, a Transwell chamber was placed into the well, and the cell density was adjusted to 1×10^6 cells/well. The cells were transfected with either STAT1/CD74 over-expressing plasmids or MIF-transfected siRNA and cultured at 37 °C for 48 h. The liquid in the culture was aspirated and the cells were washed gently with PBS and fixed with methanol for 20 min. Then, they were stained with 0.1% crystal violet at room temperature for 30 min and washed gently with PBS thrice. The cells were carefully wiped onto the upper layer of a microporous membrane with a cotton swab, and counted at 200× magnification under an inverted microscope. The cells moved to the lower layer of the microporous membrane, upon which each field was randomly counted five times and the average was taken.

Cell proliferation assay

Cells were seeded into 96-well plates at a density of 2000 cells/well and incubated at 37 °C for 1 to 5 days. Then, the cells were incubated with MTT solution (0.5 mg/mL) at 37 °C for 4 h and the medium was replaced with 150 μL DMSO. A microplate reader was used to detect the absorbance at 570 nm. All the experiments were repeated thrice independently and there were 5 samples per group.

Co-immunoprecipitation

Cell extracts were incubated with the primary antibody or normal IgG overnight at 4 °C and then incubated with Protein A/G PLUS-Agarose for 2 h at 4 °C. Thereafter, the agarose was collected and washed with lysis buffer.

Statistical methods

All the data obtained in this study were analyzed using SPSS 19.0 software. The results are presented as mean ± standard deviation; the statistical differences were determined using the *t*-test. Differences were considered significant at $P < 0.05$, $P < 0.01$, and $P < 0.001$ (NS: no sense).

Results

MIF has no significant effect on the expression of STAT1 and CD74 in colon cancer cells

First, we transfected siRNA into colon cancer cells to knockdown MIF. Then, PCR and western blot assays were performed to detect the mRNA and protein expressions of STAT1 and CD74. The results showed that MIF knockdown did not significantly change the expression of either STAT1 or CD74 compared to that in the control group ($P > 0.05$), indicating that MIF did not affect the expression of STAT1 or CD74 mRNA and protein (Fig. 1a, 1b).

MIF can promote the binding of STAT1 and CD74 proteins

In co-immunoprecipitation assays, the lysates of colon cancer cells co-transfected with MIF siRNAs and pCMV-HA-STAT1, pCMV-Myc-CD74 plasmids and those only transfected with pCMV-HA-STAT1, pCMV-Myc-CD74 plasmids were extracted. The lysates were precipitated with polyclonal antibodies of anti-Myc or pre-immune and detected with HA-monoclonal antibodies. Bands were detected for both the direct output lysate (input) and lysate precipitated by anti-Myc polyclonal antibody; however, the MIF knockdown group (siMIF) showed a significantly lower band intensity than the control group (Fig. 2). These results suggested that MIF knockdown inhibited the binding of STAT1 to CD74 protein.

MIF promotes colon cancer cell proliferation and invasion via STAT1 and CD74

The results of the Transwell assay showed that the number of cells passing through the Transwell membrane increased more significantly in the group overexpressing STAT1/CD74 and MIF knockdown than in the group that only overexpressed STAT1/CD74 (Fig. 3a, 3b). This result indicated that MIF promoted the proliferation and invasion of colon cancer cells through the STAT1/CD74 axis.

Discussion

Recurrence and metastasis are the key factors that affect the prognosis and quality of life of colon cancer patients, and have become the focus of current clinical and

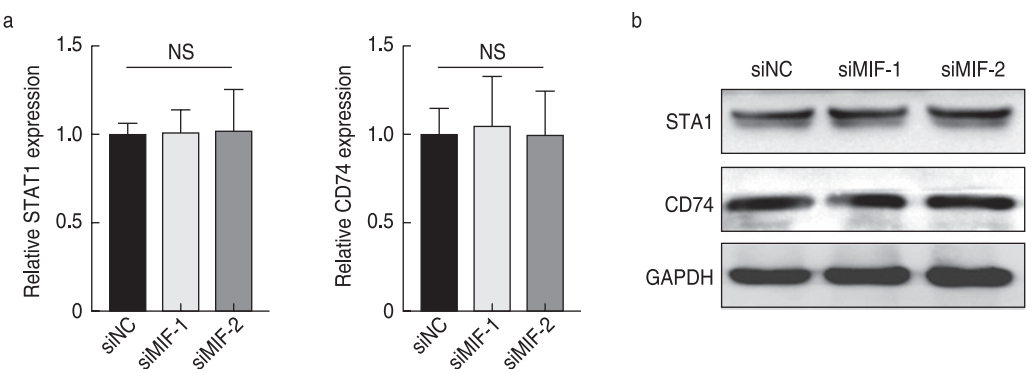

Fig. 1 MIF has no significant effect on STAT1 and CD74 mRNA (a) and protein (b) expression

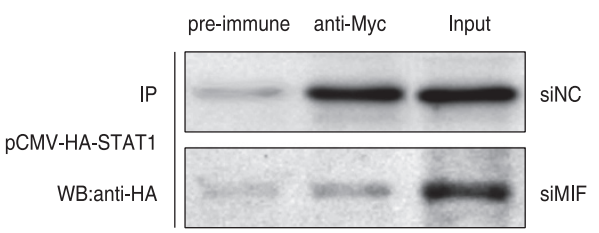

Fig. 2 Co-immunoprecipitation assay indicated that MIF knockdown inhibited CD74 and STAT1 protein combination

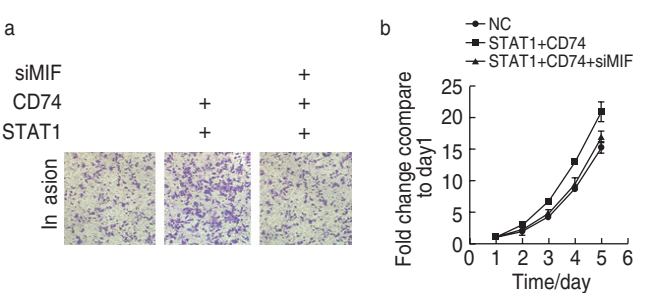

Fig. 3 MIF affects colon cancer cell invasion (a) and proliferation (b) through CD74 and STAT1

basic research. Although some progress has been made in the clinical efficacy of radiotherapy, chemotherapy, and molecular targeted therapy for colon cancer, the overall prognosis of patients still has great room for improvement. Malignant biological behaviors such as unlimited proliferation and invasion of tumor cells are important factors that promote rapid progress of colon cancer. Therefore, research focusing on the regulation of abnormally expressed genes involved in tumor cell proliferation and invasion can provide potential molecular targets and new ideas for clinical diagnosis and treatment.

MIF is stored in immune cells such as monocyte macrophages, B cells, T cells, and dendritic cells. It is also present in epithelial cells, the epithelial cytoplasm, and endocrine cells, which can promote the initiation and development of inflammatory diseases [11]. Studies have also shown that MIF is highly expressed in gliomas, prostate cancer, nasopharyngeal cancer, and colon cancer, and is involved in the regulation of tumorigenesis and cancer development. Its functional mechanism includes the inhibition of the tumor suppressive effects of p53, CD74/CD44, MAPK, or other signaling pathways that regulate tumor cell growth, apoptosis, spread, and angiogenesis [12–16].

CD74 is a membrane antigen related to MHC-II restricted antigen presentation. It exists both in the cell membrane and cytoplasm. Generally, CD74 is expressed in lymphocytes, monocytes/macrophages, Langham cells, dendritic cells, activated T lymphocytes, and some thymic epithelial cells. Studies on CD74 have mostly focused on the field of cellular immunology. Recently, however, the role and functional mechanism of CD74 in tumors has attracted the attention of many scientists. Some have reported that the expression intensity of CD74 has a negative correlation with the prognosis of patients with gastric cancer. Other studies have found that CD74 can be used as a biological molecular marker to predict the prognosis of patients with pancreatic and lung cancers. Furthermore, high expression of CD74 in colon cancer can also promote cancer development [17–21]. With regard to the functional mechanism, it has been proved that MIF interacts with the cell membrane receptor CD74; CD74 in the cytoplasmic segment can activate the nuclear transcription factor NF-κB to regulate the transcription of downstream targeted genes. MIF can also function through the interaction of CD7/CD44 to activate the Src family protein tyrosine kinase, causing ERK phosphorylation; or by regulating cell proliferation by activating Syk and the PI3K/AKT pathway [22–25]. It has been widely reported that MIF binds to the cell membrane receptor CD74 to exercise its functions. Therefore, the intracellular molecular mechanism and signaling pathway are the focus of research in this field.

STAT1 is a DNA-binding protein that can work as a nuclear transcription factor to regulate the transcription and expression of genes related to cell proliferation, invasion, and immune response, and plays an important role in the initiation and development of malignant tumors. Our previous research demonstrated that STAT1 can bind to CD74 protein in colon cancer cells. In this study, we demonstrated that MIF inhibition reduces the binding of CD74 and STAT1. Furthermore, the results of cell biology experiments showed that the proliferation and invasion ability of colon cancer cells were significantly decreases upon MIF knockdown. Therefore, we conclude that MIF regulates the malignant biological behavior of colon cancer by affecting the binding of CD74 and STAT1. Moreover, we noticed that, with regard to the tumor extracellular environment, i.e., tumor microenvironment formation and positive feedback effects, immune evasion is also an important factor for tumor recurrence and metastasis. A large number of studies have reported that MIF, CD74, and STAT1 play important roles in local or systemic inflammation-related diseases, and that their molecular interaction mechanisms are our next research directions.

In summary, MIF silencing may inhibit the proliferation, migration, and invasion of colon cancer cells. The underlying mechanism probably regulates the binding of CD74 and STAT1 proteins, thereby affecting the expression of the STAT1 pathway. This study provides new ideas for targeted treatment of colon cancer by silencing the effect of MIF expression on colon cancer cells.

Conflicts of interest

The authors indicated no potential conflicts of interest.

References

1. Siegel RL, Miller KD, Jemal A. Cancer statistics, 2020. CA Cancer J Clin, 2020, 70: 7–30.
2. Feng RM, Zong YN, Cao SM, *et al*. Current cancer situation in China: good or bad news from the 2018 Global Cancer Statistics? Cancer Commun (Lond), 2019, 39: 22.
3. Yokota J. Tumor progression and metastasis. Carcinogenesis, 2000, 21: 497–503.
4. Bernhagen J, Calandra T, Mitchell RA, *et al*. MIF is a pituitary-derived cytokine that potentiates lethal endotoxaemia. Nature, 1993, 365: 756–759.
5. Roger T, Froidevaux C, Martin C, *et al*. Macrophage migration inhibitory factor (MIF) regulates host responses to endotoxin through modulation of Toll-like receptor 4 (TLR4). J Endotoxin Res, 2003, 9: 119–123.
6. Cournia Z, Leng L, Gandavadi S, *et al*. Discovery of human macrophage migration inhibitory factor (MIF)-CD74 antagonists via virtual screening. J Med Chem, 2009, 52: 416–424.
7. Fan C, Rajasekaran D, Syed MA, *et al*. MIF intersubunit disulfide mutant antagonist supports activation of CD74 by endogenous MIF trimer at physiologic concentrations. Proc Natl Acad Sci U S A, 2013,

110: 10994–10999.
8. Leng L, Metz CN, Fang Y, *et al*. MIF signal transduction initiated by binding to CD74. J Exp Med, 2003, 197: 1467–1476.
9. Kaler P, Owusu BY, Augenlicht L, *et al*. The role of STAT1 for crosstalk between fibroblasts and colon cancer cells. Front Oncol, 2014, 4: 88.
10. Ramana CV, Gil MP, Schreiber RD, *et al*. STAT1-dependent and independent pathways in IFN-γ-dependent signaling. Trends Immunol, 2002, 23: 96–101.
11. Roger T, David J, Glauser MP, *et al*. MIF regulates innate immune responses through modulation of Toll-like receptor 4. Nature, 2001, 414: 920–924.
12. Camlica H, Duranyildiz D, Oguz H, *et al*. The diagnostic value of macrophage migration inhibitory factor (MIF) in gastric cancer. Pathol Oncol Res, 2008, 14: 79–83.
13. Lechien JR, Kindt N, Costa Pde A, *et al*. MIF in head and neck cancer: a new therapeutic target? Rev Laryngol Otol Rhinol (Bord), 2013, 134: 67–74.
14. Lin S, Wang M, Liu X, *et al*. Association of genetic polymorphisms in MIF with breast cancer risk in Chinese women. Clin Exp Med, 2017, 17: 395–401.
15. Richard V, Kindt N, Saussez S, *et al*. Macrophage migration inhibitory factor involvement in breast cancer (Review). Int J Oncol, 2015, 47: 1627–1633.
16. Rosengren E, Bucala R, Aman P, *et al*. The immunoregulatory mediator macrophage migration inhibitory factor (MIF) catalyzes a tautomerization reaction. Mol Med, 1996, 2: 143–149.
17. Bozzi F, Mogavero A, Varinelli L, *et al*. MIF/CD74 axis is a target for novel therapies in colon carcinomatosis.J Exp Clin Cancer Res, 2017, 36: 16.
18. Cheng SP, Liu CL, Chen MJ, *et al*. CD74 expression and its therapeutic potential in thyroid carcinoma. Endocr Relat Cancer, 2015, 22: 179–190.
19. McClelland M, Zhao L, Carskadon S, *et al*. Expression of CD74, the receptor for macrophage migration inhibitory factor, in non-small cell lung cancer. Am J Pathol, 2009, 174: 638–646.
20. Metodieva G, Nogueira-de-Souza NC, Greenwood C, *et al*. CD74-dependent deregulation of the tumor suppressor scribble in human epithelial and breast cancer cells. Neoplasia, 2013, 15: 660–668.
21. Nagata S, Jin YF, Yoshizato K, *et al*. CD74 is a novel prognostic factor for patients with pancreatic cancer receiving multimodal therapy. Ann Surg Oncol, 2009, 16: 2531–2538.
22. Baron N, Deuster O, Noelker C, *et al*. Role of macrophage migration inhibitory factor in primary glioblastoma multiforme cells. J Neurosci Res, 2011, 89: 711–717.
23. Becker-Herman S, Arie G, Medvedovsky H, *et al*. CD74 is a member of the regulated intramembrane proteolysis-processed protein family. Mol Biol Cell, 2005, 16: 5061–5069.
24. Shi X, Leng L, Wang T, *et al*. CD44 is the signaling component of the macrophage migration inhibitory factor-CD74 receptor complex. Immunity, 2006, 25: 595–606.
25. Leng L, Bucala R. Insight into the biology of macrophage migration inhibitory factor (MIF) revealed by the cloning of its cell surface receptor. Cell Res, 2006, 16: 162–168.

DOI 10.1007/s10330-020-0419-9
Cite this article as: Liu F, Zhong JX, Sun JB, *et al*. Effects of MIF on proliferation, migration, and STAT1 pathway of colon cancer cells. Oncol Transl Med, 2020, 6: 121–125.

Oncology and Translational Medicine
DOI 10.1007/s10330-020-0416-6

June 2020, Vol. 6, No. 3, P126–P130

ORIGINAL ARTICLE

Assessing anxiety, depression, and stress among inpatients with cancer*

Honghong Xu[1], Ruotong Xue[1], Yi Cheng[2], Yujie Zhang[2], Jie Rao[2], Mei Liu[2], Shiying Yu[2], Lingxiang Liu[3], Yiqian Liu[3], Yongqian Shu[3], Liuqing Yang[4], Hanping Shi[4] (✉)

[1] Medical Psychology Department, Peking University Health Science Center, Beijing 100191, China
[2] Department of Oncology, Tongji Hospital, Tongji Medical College, Huazhong University of Science and Technology, Wuhan 430030, China
[3] Department of Oncology, First Affiliated Hospital of Nanjing Medical University, Nanjing 210029, China
[4] Department of Gastrointestinal Surgery, Department of Clinical Nutrition, Beijing Shijitan Hospital, Capital Medical University, Beijing 100038, China

Abstract

Objective This study aimed to assess anxiety, depression, and stress among inpatients with cancer.

Methods Two hundred thirty-five hospitalized patients with cancer were surveyed with the Depression Anxiety Stress Scales (simplified Chinese Version). The software program SPSS 25.0 was used for statistical analysis of the survey data.

Results The average scores of depression, anxiety, and stress of inpatients with cancer were 12.17, 11.84, and 13.98 respectively, which were higher than the normal range. The scores of anxiety and stress of inpatients with different caregivers were statistically different (P = 0.024/0.036). The anxiety and stress scores of inpatients with spouses as caregivers were higher than those of inpatients with children as caregivers. There was a statistically significant difference in the incidence of stress between inpatients with cancer with religious beliefs and inpatients with cancer without religious beliefs (P = 0.026), and those with religious beliefs had greater incidence of stress. The score of anxiety was significantly higher for inpatients with children than for inpatients without children (P = 0.040).

Conclusion The anxiety, depression, and stress levels of inpatients with cancer are relatively high. It is necessary to pay special attention to the psychological status of these patients during clinical diagnosis and treatment to improve their quality of life.

Received: 9 April 2020
Revised: 4 May 2020
Accepted: 16 May 2020

Key words: inpatients with cancer; anxiety; depression; stress

Cancer is the second leading cause of death globally, and was responsible for an estimated 9.6 million deaths in 2018. Globally, about one in six deaths is due to cancer. Cancer affects not only physiological function but also mental health [1–2]. However, psychological factors can also affect the occurrence and development of the physical disease [3]. Anxiety and depression are highly prevalent in patients with cancer. They are caused by factors such as pain, fatigue, social loneliness, interpersonal relationship disorders, fear of tumor recurrence, and death. The inability to continue to assume social roles and the economic problems caused by treatment also place patients with cancer at a high risk for stress. These mental health problems may affect the ability of patients to cope with cancer and have a negative impact on the effectiveness of treatment. This study aimed to assess anxiety, depression, and stress among inpatients with cancer and to explore related factors. The findings of this study can provide a better and more comprehensive understanding of the psychological status of patients with

✉ Correspondence to: Hanping Shi. Email: shihp@vip.163.com
* Supported by a grant from the National Key Research and Development Program: the Key Technology of Palliative Care and Nursing for Cancer Patients (No. 2017YFC1309200).

cancer and inform future psychological interventions.

Materials and methods

Participants

The participants were 235 patients with cancer treated in the inpatient department of Tongji Hospital (affiliated with Huazhong University of Science and Technology and the First Affiliated Hospital of Nanjing Medical University) from October 2019 to November 2019.

Inclusion criteria were as follows: (1) Inpatients diagnosed with cancer by pathology/cytology, clinical, and imaging studies; (2) Aged 18 years or over; (3) Able and willing to participate; (4) Survival period ≥ 3 months.

Exclusion criteria were as follows: (1) Those who were unable to complete the study due to illness and (2)Those with cognitive impairment or a history of mental illness.

Research tools

(1) A demographic characteristics questionnaire was specifically developed for the study. The questionnaire was used to collect data on age, gender, occupation, marital status, parental status, economic status, religious beliefs, and more. (2) A disease status questionnaire was also developed for the study and was used to collect data on the main period of illness, caregivers, diagnosis of diseases, treatment type, etc. The Depression Anxiety Stress Scales (DASS-21) (simplified Chinese version) was used to measure depression, anxiety, and stress. The DASS-21 consists of 21 items, which are divided into 3 subscales: depression, anxiety, and stress. Each subscale consists of 7 items. Responses are based on a 4-point scale (from 0 to 3 points, 0 =”Did not apply to me at all,” 1 =”Applied to me to some degree, or some of the time,” 2 =Applied to me to a considerable degree or a good part of the time, and “ 3 =”Applied to me very much or most of the time”). A higher score indicates a higher level of anxiety, depression, or stress. Recommended cut-off scores for conventional categories of severity (normal, moderate, severe) are presented in Table 1.

Test procedures and ethical considerations

Testers who had undergone training to standardize the test procedures explained the study’s purpose and procedure to the patients. After informed consent was obtained from a patient, the patient filled out the questionnaire, which was collected by the testers.

Table 1 Cut-off scores of DASS-21

	Depression	Anxiety	Stress
Normal	0–9	0–7	0–14
Mild	10–13	8–9	15–18
Moderate	14–20	10–14	19–25
Severe	21–27	15–19	16–33
Extremely severe	28+	20+	34+

Statistical methods

The software program SPSS 25.0 (IBM Corp., Armonk, NY, USA) was used for statistical analysis of the data. Descriptive statistics were used to analyze the general characteristics of the patients. The independent sample *t* test and chi-square test were used to determine whether the binary variables (sex, religion, children, and hospital admissions) affected the patient’s questionnaire scores and indicators were normal. Univariate analysis of variance and the chi-square test were used to analyze the effect of disordered variables (marital status, caregivers, knowledge level, and diagnosis type) on the questionnaire scores and indicators. The Kruskal-Wallis H test was used to determine the impact of economic status on stress, depression, and anxiety levels.

Results

Demographic characteristics of the participants

A total of 235 questionnaires were returned, of which 232 were found to be valid. Of all the respondents, 132 (56.9%) were male and 100 (43.1%) were female. The patients’ ages ranged from 22 to 83 years. With regard to marital status, 6 (2.6%) weJre unmarried, 217 (93.5%) were married, 2 (0.9%) were divorced, and 7 (3.0%) were widowed. Two hundred twenty-five (97.0%) had children and 7 (3.0%) had no children. One hundred forty-two (61.2%) were provided care by their spouses, 65 (28.0%) by their children, 2 (0.9%) by a nursing assistant, and 23 (9.9%) by other individuals. With regard to occupational status, 33 (14.2%) were farmers, 32 (13.8%) were non-agricultural workers, and 28 (12.1%) were unemployed. In terms of family income, 89 (38.4%) patients had annual family incomes below 50,000 yuan, 89 (38.4%) between 50,000 and 100,000 yuan, 36 (15.5%) between 100,000 and 200,000 yuan, 12 (5.2%) between 200,000 and 300,000 yuan, and 6 (2.6%) with incomes of over 300,000 yuan. In terms of religious beliefs, 18 (7.8%) patients practiced Buddhism, 4 (1.7%) practiced Christianity, 3 (1.3%) practiced a religion besides Buddhism or Christianity, and 207 (89.2%) held no religious beliefs. Twenty-eight people (12.1%) knew nothing about the diagnosis and treatment plan of the current disease, 160 (69%) had some knowledge, and 44 (19.0%) had a high level of knowledge. With regard to cancer type, 131 (56.5%) patients were diagnosed with lung cancer, 13 (5.6%) with esophageal cancer, 5 (2.2%) with pancreatic cancer, and 83 with other cancers. Forty-four (19.0%) were hospitalized for the first time, and 188 (81.0%) were admitted for the second time or more.

Analysis of DASS-21 survey results

Depression, anxiety, and stress scores

The average scores of the depression, anxiety, and stress subscales of the DASS-21 were 12.17 ± 10.13 points, 11.84 ± 8.74 points, and 13.98 ± 9.74 points. respectively. The overall scores for depression and anxiety were beyond normal range, and the overall scores of the patients showed mild depression and moderate anxiety. Although the overall stress score was within normal range (0–14 points), it was close to the upper limit. Among the three subscales, 151 patients (65.1%) showed higher scores in anxiety than the normal range, 124 (53.4%) showed higher scores in depression, and 83 (35.8%) in stress (Table 2).

Analysis of DASS-21 scores by caregiver type

A one-way analysis of variance was used to compare the average scores of depression, anxiety, and stress of patients by caregiver type. The results showed that patients with different types of caregivers had statistically significant differences in anxiety and stress scores ($P< 0.05$). Then the T3 method was used for subsequent post-examination. The results showed that the score of stress of patients with spouses as caregivers (15.34 ± 10.21) was higher than that of patients with children as caregivers (11.23 ± 6.80), and the difference was statistically significant ($P= 0.005$). The anxiety score of patients with spouses as caregivers (13.20 ± 9.08) was higher than that of patients with children as caregiver (9.29 ± 6.59), and the difference was statistically significant ($P= 0.004$) (Table 3).

Differences in stress level between patients with and without religious beliefs

Stress level was further divided into two categories: normal (0-14 points) and abnormal (greater than 14 points). The chi-square test was used to analyze the differences in stress level between patients with and without religious beliefs. No difference was found between patients with religious beliefs and non-religious beliefs in terms of normal stress levels. The Pearson chi-square value was 4.988, and the P value was 0.026, indicating that patients with religious beliefs and non-religious beliefs differ in terms of incidence of abnormal stress. Patients with religious beliefs were found to have high incidence of abnormal stress (Table 4).

Differences in anxiety level between patients with and without children

Anxiety level was further divided into two categories: normal (0-7 points) and abnormal (greater than 7 points). The chi-square test was used to analyze the differences in anxiety between patients with and without children. No difference was found between patients with and without children in terms of normal anxiety levels. The Pearson chi-square value was 4.235, and the P value was 0.040, indicating that patients with children and without children differ in terms of incidence of abnormal anxiety. Patients with children were found to have high incidence of abnormal anxiety (Table 5).

Discussion

In the research on the occurrence, progress, and prognosis of cancer, the role played by psychosocial factors has been receiving more and more attention. The treatment of cancer has also changed from simple anti-tumor drug treatment to comprehensive treatment that combines both physical and psychological approaches. The goal of treatment is mainly to improve the survival rate and improve the patient's quality of life. Studies conducted in China and abroad have confirmed that patients with cancer have different degrees of emotional disorders, and that emotional disorders can affect the rehabilitation and prognosis of patients [4–5]. Li Jun [6] and

Table 2 Distribution of DASS-21 in 232 cancer patients (%)

	Depression	Anxiety	Stress
Normal	108 (46.6)	81 (34.9)	149 (64.2)
Mild	31 (13.4)	21 (9.1)	26 (11.2)
Moderate	56 (24.1)	63 (27.2)	25 (10.8)
Severe	15 (6.5)	24 (10.3)	17 (7.3)
Extremely severe	22 (9.5)	43 (18.5)	15 (6.5)

Table 3 DASS-21 scores of patients with different caregivers ($\chi \pm s$)

Caregiver	*n*	Depression	Anxiety	Stress
Spouse	142	13.34 ± 10.47	13.20 ± 9.08	15.34 ± 10.21
Children	65	9.42 ± 7.24	9.29 ± 6.59	11.23 ± 6.80
Nursing assistant	2	9.00 ± 12.73	10.00 ± 14.14	9.00 ± 12.73
Other	23	13.04 ± 13.46	10.78 ± 10.23	13.83 ± 12.25
F		2.399	3.217	2.892
P		0.069	0.024	0.036

Table 4 Comparison of stress status between patients with and without religious belief (Numbers of participants)

Religious Belief	Stress		Total
	Normal	Abnormal	
Without	138	69	207
With	11	14	25
Total	149	83	232

Table 5 Comparison of the anxiety level of patients with or without children (Numbers of participants)

Children	Anxiety		Total
	Normal	Abnormal	
Without	76	149	225
With	5	2	7
Total	81	151	232

others have found a positive rate of depression in patients with malignant tumors of 58.9%, a positive rate of anxiety of 28.1%, and a relatively high stress level [7].

The DASS-21 is a short version of the DASS-42, which was originally used to investigate the depression, anxiety, and stress status of normal adults based on their experienced emotions within the past week. Previous research has demonstrated that the Chinese version of the DASS-21 is highly reliable and valid, and can effectively be used to assess levels of negative emotions [8]. The scale is easy to use and is suitable for clinical and scientific research. In the present study, 65.1% of inpatients with cancer showed different anxiety levels, 53.4% of patients had depression beyond the normal range, and 35.8% of patients had higher stress than the general population.

The present study also showed that patients under the care of their spouses have higher levels of anxiety and stress compared with those under the care of their children ($P < 0.05$). The possible explanations for this finding are as follows: If the patient is a middle-aged or young person, their spouse will have different degrees of influence on their jobs, which will affect the family income. If there are still minors in the family who need care, anxiety and stress levels are likely to increase. If the patient is an older adult, the spouse is also likely to be an older adult. Although there is no burden of occupation due to the spouse's age, long-term and complicated care work may cause stress and anxiety in the patient and caregiver.

In addition, incidence of anxiety among patients with children was found to be higher than that among patients without children. This finding may be because patients with children worry that they cannot effectively fulfill their role as parents (e.g., properly care for their children and accompany their children) and that they may burden their children.

There is no conclusive evidence of the influence of religious beliefs on mental health of patients. Ding Zhihong [9] has shown that religious beliefs play an important role in improving the incidence of depression in the elderly, and Peng Ling *et al* [10] has demonstrated that there is no statistical difference in depression and anxiety between patients with cancer with and without religious beliefs. However, the differences in quality of life have been found to be statistically significant. The results of the present study showed that patients with religious beliefs have a higher incidence of abnormal stress than patients without religious beliefs. This finding may be because patients with cancer may question their religious and spiritual beliefs during their illness. However, because only 105 of the participants in the study had specific religious beliefs, future studies with larger samples may be needed.

With regard to the relationship between gender, age, marital status, and cancer type, and the psychological status of patients, the findings are controversial. Zhang Yening [11] showed that there are differences in psychological pain between male and female patients with cancer; female patients are more likely to suffer from mental distress. Zabora [12] showed that unmarried patients with lung cancer have the highest rates of mental distress. The results of the present study indicated that gender, age, marital status, and cancer type are not related to patients' anxiety, depression, and stress levels. These findings are consistent with those of a Korean study conducted by Shim [13].

With regard to the relationship between annual family income and the psychological symptoms of patients, previous studies [14] have shown that patients with low income (low social economic status) have more severe mental problems. The present study found no significant differences in depression, anxiety, and stress between patients with different annual family incomes. This finding may be related to China's deepening of medical insurance system reform in recent years, which has led to an increase in the proportion of patients receiving reimbursement for treatment. The impact of family economic status on psychological status may have been reduced through the reforms. In addition, in the present study, anxiety, depression, and stress levels were not found to be associated with the number of hospital admissions. This finding is consistent with those of a study by Li Jun [6].

This study had several limitations. First, because of the limited sample size, in some aspects, the comparison between groups did not show the significance of the difference. Second, because only the DASS was used, other in-depth psychological factors were not investigated. Therefore, future studies with larger sample sizes and a variety of tools should be conducted, in order to deeply explore the influencing factors of the mental health of patients with cancer.

In conclusion, this study found that among hospitalized patients with cancer, the incidence of depression, anxiety, and stress are relatively high, and for some patients, the levels are extremely high. In the clinical diagnosis and treatment of patients with cancer, attention should be paid to appropriate psychological counseling and intervention, in order to improve psychological health and quality of life among these patients.

Conflicts of interest

The authors indicated no potential conflicts of interest.

References

1. Ferlay J, Parkin DM, Steliarova-Foucher E. Estimates of cancer incidence and mortality in Europe in 2008. Eur J Cancer, 2010, 46:

765–781.
2. Jemal A, Bray F, Center MM, *et al*. Global cancer statistics. CA Cancer J Clin, 2011, 61: 69–90.
3. Lu M, Xu HF, Xia YY. Anxiety and depression of cancer patients. Chin Mental Health J (Chinese), 1999, 13: 187.
4. Mssise MJ, Holland JC. Depression and the cancer patient. Clin Psychiatry, 1990, 51: 12.
5. Li JZ, Wu AQ, Wu CY. Study on the correlation between emotional disorder and psychosocial factors of tumor patients. Chin J Behav Med Sci (Chinese), 2001,10: 545–547.
6. Li J, Li YL, Xie YX. Clinical investigation and analysis of depression and anxiety in patients with malignant tumors. J Chin Physician (Chinese), 2009, 11: 1003–1005.
7. Zhang YH, Jiang H, Suzuki Zhijinzhi, *et al*. A survey of the status of stress coping ability of cancer patients. Chin J Nurs (Chinese), 2006, 41: 898–901.
8. Gong X, Xie XY, Xu R, *et al*. Psychometric properties of the Chinese versions of DASS-21 in Chinese college students. Chin J Clin Psychol (Chinese), 2010, 18: 443–446.
9. Ding ZH. The effect of religious belief on reducing depression of Chinese elderly. Chin J Gerontol (Chinese), 2014, 34: 181–183.
10. Peng L, Zheng XQ, Cai FM. Survey and analysis on characteristics of religious belief for cancer patients and its influence on their psychology and quality of life. Nurs Rehabil (Chinese), 2018, 17: 15–21.
11. Zhang YN, Zhang HW, Song LL, *et al*. Application of psychological pain thermometer in screening for psychological pain of Chinese cancer patients. Chin J Mental Health (Chinese), 2010, 24: 897–902.
12. Zabora J, Brintzenhofeszoc K, Curbow B, *et al*. The prevalence of psychological distress by cancer site. Psychooncology, 2001, 10: 19–28.
13. Shim EJ, Shin YW, Jeon HJ, *et al*. Distress and its correlates in Korean cancer patients: pilot use of the distress thermometer and the problem list. Psychooncology, 2008, 17: 548–555.
14. Carlson LE, Angen M, Cullum J, *et al*. High levels of untreated distress and fatigue in cancer patients. Br J Cancer, 2004, 90: 2297–2304.

DOI 10.1007/s10330-020-0416-6
Cite this article as: Xu HH, Xue RT, Cheng Y, *et al*. Assessing anxiety, depression, and stress among inpatients with cancer. Oncol Transl Med, 2020, 6: 126–130.

Oncology and Translational Medicine
DOI 10.1007/s10330-020-0409-9

June 2020, Vol. 6, No. 3, P131–P133

CASE REPORT

A case report of double-protein expression in primary uterine cervical diffuse large B cell lymphoma and a review of the literature

Xiaoying Quan[1] (✉), Zhihui Zhang[2]

[1] Department of Medical Oncology, the Sixth People's Hospital of Chengdu, Chengdu 610051, China
[2] Department of Lymphoma, Sichuan Cancer Hospital and Research Institute, Chengdu 610041, China

Abstract

Primary non-Hodgkin's lymphoma of the uterine cervix is rarely observed. Here, we report a case of "double-protein" expression in a primary uterine cervical diffuse large B-cell lymphoma that was detected based on cervical biopsies at Sichuan Cancer Hospital in December 2016 in a 53-year-old woman with a 1-month history of postmenopausal vaginal bleeding. She was diagnosed with stage IVA cervical cancer after workup and treated with six cycles of rituximab + cyclophosphamide + epirubicin + vindesine + prednisone. She showed a positive partial response after two cycles; however, response assessment revealed a progressive disease after six cycles. Based on the current condition, a treatment regimen comprising a combination of second-line chemotherapy and radiotherapy was advised for the patient. Unfortunately, she discontinued her treatment because of various factors. We conclude that "double-protein" expression in primary uterine cervical diffuse large B-cell lymphoma is difficult to treat and has a poor prognosis. Therefore, improving the diagnosis and treatment of this disease should be considered.

Received: 12 March 2020
Revised: 22 April 2020
Accepted: 15 May 2020

Key words: diffuse large B-cell lymphoma; uterine cervix; "double-protein" expression

Non-Hodgkin's lymphoma (NHL) involves the extranodal regions in approximately one-third of patients [1]. The most common extranodal sites are the gastrointestinal tract, nasal cavity, and skin. However, female genital tract lymphoma is an extremely rare disease, which accounts for 1.5% of extranodal NHL [2], and its clinical manifestation includes a lack of specificity, leading to misdiagnosis. A previous study identified that the most common subtype of uterine cervical lymphoma is diffuse large B-cell lymphoma (DLBCL), with abnormal vaginal bleeding being the most common presenting symptom [3]. DLBCL is a clinically and biologically heterogeneous disease and could be divided into prognostically important subgroups: germinal center subtype (GCB) and non-GCB [4]. Hence, the response of patients to therapy invariably differs. Currently, there is a growing interest in "double-protein" lymphoma that is defined as the co-expression of two oncogenes (MYC and BCL2 and/or BCL6) [5]. A recent study identified that MYC/BCL2 co-expression was a predictor of prognosis in DLBCL patients treated with rituximab + cyclophosphamide + epirubicin + vindesine + prednisone (R-CHOP) chemotherapy because most treatment failures were observed in "double-protein" DLBCL [6]. Therefore, a standard treatment has not yet been established. Here, we report a case of DLBCL with "double-protein" expression involving the uterine cervix treated with R-CHOP chemotherapy.

Case presentation

A 53-year-old postmenopausal woman presented with a 1-month history of vaginal bleeding, with the absence of fever, weight loss, night sweats, and an Eastern Cooperative Oncology Group performance status score of 1. She subsequently visited the Department of Obstetrics and Gynecology in our hospital. Gynecological examination showed a large exophytic mass in the cervix with necrotic and bleeding areas infiltrating the upper vagina and left parametria.

A cervical biopsy revealed a high-grade non-Hodgkin's DLBCL, GCB, and double-protein expression. Immunohistochemistry revealed the following results: creatine kinase (–), cluster of differentiation CD3 (–), CD5

✉ Correspondence to: Xiaoying Quan. Email: 1193084163@qq.com

(–), CD10 (+), CD30 (–), CD20 (+), Lens culinaris lectin (+), PAX5 (+), myeloperoxidase (–), CD79a (+), CD138 (–), epithelial membrane antigen (–), vimentin (–), MUM-1 (–), BCL2 (+, 40%), BCL6 (–), c-MYC (+, 60%), P53 (–), EBER (–), and Ki-67 (+, 80%).

Contrast-enhanced magnetic resonance imaging (MRI) of the upper abdomen and pelvis revealed a solid tumor (4.9 × 6.1 × 4.0 cm) occupying the uterine cervix, extending to the upper part of the vagina and the left parametria. Multiple lymph nodes in the subcutaneous fat layer of the upper left abdominal wall, right perirenal space, left iliac fossa, presacral space, right rectum, and left inguinal groin were enlarged (largest 2.1 × 2 cm) (Fig. 1).

Contrast-enhanced computed tomography (CT) of the neck and chest revealed no evidence of lymphoma (figure not shown). Bone marrow and cerebrospinal fluid were uninvolved. Routine laboratory analysis showed an elevated serum lactate dehydrogenase level (174 U/L [normal value, 0–240 U/L]). Viral serological results for human immunodeficiency virus, hepatitis B surface antigen, hepatitis C, and syphilis were negative. Based on the clinical and imaging examination findings, the patient was diagnosed with DLBCL (GCB, BCL2/c-MYC double-protein expression, stage IVA, IPI score of 2).

She originally planned to receive six cycles of 3-weekly R-CHOP chemotherapy followed by involved-field radiotherapy. After two cycles, an MRI of the upper abdomen and pelvis revealed a positive partial response in all lesions (Fig. 2). After four cycles, an MRI revealed a stable disease (Fig. 3). After the completion of six cycles, an MRI revealed the progression of the cervical mass (Fig. 4). Meanwhile, contrast-enhanced chest CT revealed a lymphoma of the right breast (Fig. 5), which was confirmed by a lumpectomy of the right breast. Her family refused involved-field radiotherapy and second-line chemotherapy because of various factors. Finally, she discontinued treatment.

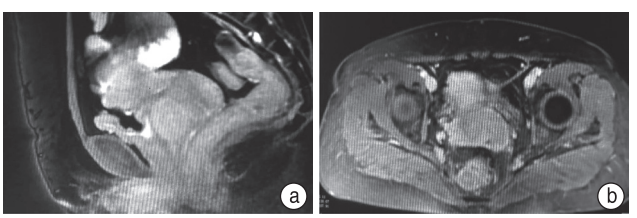

MRI scan pretreatment

Fig. 1 Contrast enhanced magnetic resonance imaging (MRI) of pelvic scan pretreatment shows that enhancing lesion is seen involving the cervix and invading the left parametria. (a) sagittal; (b) coronal

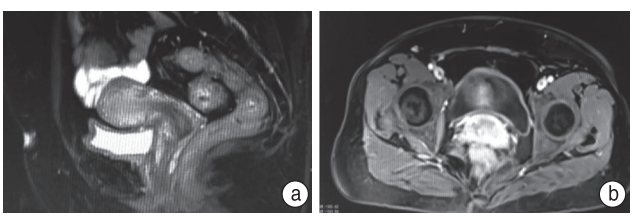

MRI scan after two cycles

Fig. 2 Contrast enhanced MRI scan after two cycles of chemotherapy showed partial response of the cervical mass and its extensions. (a) sagittal; (b) coronal

Discussion

A lymphoma can occur in every tissue; however, a primary lymphoma of the uterine cervix is a rare disease. Most cases of lymphoma have nonspecific clinical symptoms, such as vaginal bleeding, perineal discomfort, and persistent vaginal discharge. Moreover, signs of lymphoma are similar to uterine cervical cancer [1, 3]. Therefore, establishing the diagnosis of lymphoma is considered difficult, and it is often misdiagnosed because of its rarity and non-specific clinical presentation.

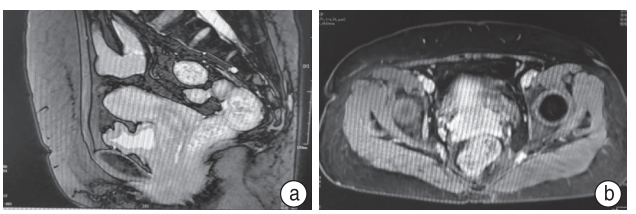

MRI scan after four cycles

Fig. 3 Contrast enhanced MRI scan after four cycles of chemotherapy showed stable disease of the cervical mass. (a) sagittal; (b) coronal

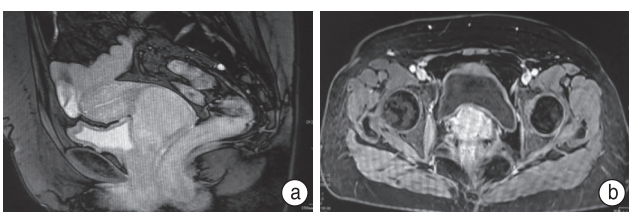

MRI scan after six cycles

Fig. 4 Contrast enhanced MRI scan after six cycles of chemotherapy progressive disease of the cervical mass. (a) sagittal; (b) coronal

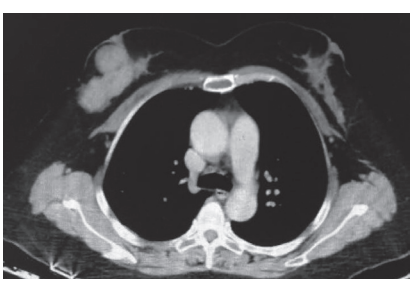

Fig. 5 Contrast enhanced CT of chest scan showed lymphoma of the right breast (coronal)

Primary cervical lymphoma is predominantly observed in postmenopausal women, and the median age of patients diagnosed with stage III or IV cervical lymphoma is 58 years (range, 22–75 years) [7]. Our patient was a 53-year-old postmenopausal woman with abnormal vaginal bleeding without evidence of B symptoms. As concluded in a previous study, the disease was confirmed by cervical biopsy, and occasionally, repeat biopsies may be required to prove the definitive diagnosis [8], similar to our case. In our study, a contrast-enhanced CT of the neck and chest revealed that the bone marrow and cerebrospinal fluid were uninvolved. However, a contrast-enhanced MRI revealed a solid tumor occupying the uterine cervix, extending to the adjacent tissue and organs. Hence, in this case report, the patient was diagnosed with primary uterine cervical DLBCL with "double-protein" expression defined by immunohistochemistry. Generally, cervical lymphoma has a good prognosis, and the 5-year survival rates of patients with early-stage and high-stage cervical lymphomas are 83% and 29%, respectively [7]. Although the optimal treatment of this condition remains unknown, patients diagnosed with cervical lymphoma can select chemotherapy, radiotherapy, and surgery, alone or in combination [9–10]. To date, according to some reported studies, the R-CHOP regimen chemotherapy followed by radiotherapy has been recommended [11]. Consistent with a previous study, in the present case report, the patient received R-CHOP chemotherapy. Unexpectedly, after the patient completed the six cycles, she showed progressive disease of the primary cervical lesion, and a clinically detectable lymphoma was observed in the right breast, which was confirmed by lumpectomy of that breast. Some explanations have significant prognostic effects as follows: (1) the patient was diagnosed with stage IVA cervical cancer with a heavy tumor load associated with poor survival, as concluded in a previous study. (2) the histological subtype showed a lymphoma with "double-protein" expression. Several groups have shown that the "double-protein" lymphoma has a poor prognosis with R-CHOP chemotherapy [12–15]. We can conclude that the co-expression of MYC and BCL-2 was significantly associated with the poor outcome.

Conclusion

In summary, a primary cervical "double-protein" expression lymphoma is a rare disease, which has a poor clinical outcome. Improving the recognition of the disease, establishing the accurate diagnosis of the disease, and initiating a timely therapy are considered important in the treatment of a cervical lymphoma. For "double-protein" expression DLBCL, the standard treatment is not yet established. Therefore, a novel treatment for patients diagnosed with DLBCL is urgently required.

Conflicts of interest

The authors indicated no potential conflicts of interest.

References

1. Baijal G, Vadiraja BM, Fernandes DJ, *et al*. Diffuse large B-cell lymphoma of the uterine cervix: a rare case managed novelly. J Cancer Res Ther, 2009, 5: 140–142.
2. Basta M, Andrawes AAR. Female genital tract lymphoma: a review of diagnosis and management. Social Science Research Network, 2009, DOI: 0.2139/ssrn.1423785.
3. Chan JK, Loizzi V, Magistris A, *et al*. Clinicopathologic features of six cases of primary cervical lymphoma. Am J Obstet Gynecol, 2005, 193: 866–872.
4. Swerdlow SH, Campo E, Pileri SA, *et al*. The 2016 revision of the World Health Organization classification of lymphoid neoplasms. Blood, 2016, 127: 2375–2390.
5. Horn H, Ziepert M, Becher C, *et al*. MYC status in concert with BCL2 and BCL6 expression predicts outcome in diffuse large B-cell lymphoma. Blood, 2013, 121: 2253–2263.
6. O'Malley DP, Auerbach A, Weiss LM. Practical applications in immunohistochemistry: evaluation of diffuse large B-cell lymphoma and related large B-cell lymphomas. Arch Pathol Lab Med, 2015, 139: 1094–1107.
7. Vang R, Medeiros LJ, Ha CS, *et al*. Non-Hodgkin's lymphomas involving the uterus: a clinicopathologic analysis of 26 cases. Mod Pathol, 2000, 13: 19–28.
8. Van Renterghem N, De Paepe P, Van den Broecke R, *et al*. Primary lymphoma of the cervix uteri: a diagnostic challenge. Report of two cases and review of the literature. Eur J Gynaecol Oncol, 2005, 26: 36–38.
9. Harris NL, Scully RE. Malignant lymphoma and granulocytic sarcoma of the uterus and vagina. A clinicopathologic analysis of 27 cases. Cancer, 1984, 53: 2530–2545.
10. Grace A, O'Connell N, Byrne P, *et al*. Malignant lymphoma of the cervix. An unusual presentation and a rare disease. Eur J Gynecol Oncol, 1999, 20: 26–28.
11. Stroh EL, Besa PC, Cox JD, *et al*. Treatment of patients with lymphomas of the uterus or cervix with combination chemotherapy and radiation therapy. Cancer, 1995, 75: 2392–2399.
12. Wang XJ, Medeiros LJ, Lin P. *et al*. MYC cytogenetic status correlates with expression and has prognostic significance in patients with MYC/BCL2 protein double-positive diffuse large B-cell lymphoma. Am J Surg Pathol, 2015, 39: 1250–1258.
13. Zhou M, Wang J, Ouyang J, *et al*. MYC protein expression is associated with poor prognosis in diffuse large B cell lymphoma patients treated with RCHOP chemotherapy. Tumour Biol, 2014, 35: 6757–6762.
14. Petrich AM, Nabhan C, Smith SM. MYC-associated and double-hit lymphomas: a review of pathobiology, prognosis, and therapeutic approaches. Cancer, 2014, 120: 3884–3895.
15. Schmidt MT, Huang Q, Alkan S. Aggressive B-cell lymphomas: a review and practical approach for the practicing pathologist. Adv Anat Pathol, 2015, 22: 168–180.

DOI 10.1007/s10330-020-0409-9
Cite this article as: Quan XY, Zhang ZH. "Double-protein" expression in primary uterine cervical diffuse large B-cell lymphoma: A case report. Oncol Transl Med, 2020, 6: 131–133.

中国科技核心期刊

（中国科技论文统计源期刊）

收录证书

CERTIFICATE OF SOURCE JOURNAL

FOR CHINESE SCIENTIFIC AND TECHNICAL PAPERS AND CITATIONS

ONCOLOGY AND TRANSLATIONAL MEDICINE

经过多项学术指标综合评定及同行专家评议推荐，贵刊被收录为“中国科技核心期刊”（中国科技论文统计源期刊）。

特颁发此证书。

中国科学技术信息研究所

Institute of Scientific and Technical Information of China

北京复兴路 15 号 100038　　www.istic.ac.cn

2019年11月

证书编号：2018-G616-0094

有效期至：2020年12月

Call For Papers
Oncology and Translational Medicine

(CN 42-1865/R, ISSN 2095-9621)

Dear Authors,

Oncology and Translational Medicine (OTM), a peer-reviewed open-access journal, is very interested in your study. If you have unpublished papers in hand and have the idea of making our journal a vehicle for your research interests, please feel free to submit your manuscripts to us via the Paper Submission System.

Aims & Scope

- Lung Cancer
- Liver Cancer
- Pancreatic Cancer
- Gastrointestinal Tumors
- Breast Cancer
- Thyroid Cancer
- Bone Tumors
- Genitourinary Tumors
- Brain Tumor
- Blood Diseases
- Gynecologic Oncology
- ENT Tumors
- Skin Cancer
- Cancer Translational Medicine
- Cancer Imageology
- Cancer Chemotherapy
- Radiotherapy
- Tumors Psychology
- Other Tumor-related Contents

Contact Us
Editorial office of Oncology and Translational Medicine
Tongji Hospital
Tongji Medical College
Huazhong University of Science and Technology
Jie Fang Da Dao 1095
430030 Wuhan, China
Tel.: 86-27-69378388
Email: dmedizin@tjh.tjmu.edu.cn;
dmedizin@sina.com

Oncology and Translational Medicine (OTM) is sponsored by Tongji Hospital, Tongji Medical College, Huazhong University of Science and Technology, China (English, bimonthly).

OTM mainly publishes original and review articles on oncology and translational medicine. We are working with the commitment to bring the highest quality research to the widest possible audience and share the research work in a timely fashion.

Manuscripts considered for publication include regular scientific papers, original research, brief reports and case reports. Review articles, commentaries and letters are welcome.

About Us

- Peer-reviewed
- Rapid publication
- Online first
- Open access
- Both print and online versions

For more information about us, please visit:
http://otm.tjh.com.cn